

Generic Loop Effects of New Scalars and Fermions in $b \rightarrow s\ell^+\ell^-$, $(g - 2)_\mu$ and a Vector-like 4th Generation

Pere Arnan^a, Andreas Crivellin^b, Marco Fedele^a, and Federico Mescia^a

^a*Departament de Física Quàntica i Astrofísica (FQA), Institut de Ciències del Cosmos (ICCUB), Universitat de Barcelona (UB), Spain*

^b*Paul Scherrer Institut, CH-5232 Villigen PSI, Switzerland*

E-mail: arnan@ub.edu, andreas.crivellin@cern.ch,
marco.fedele@icc.ub.edu, mescia@ub.edu

ABSTRACT: In this article we investigate in detail the possibility of accounting for the $b \rightarrow s\ell^+\ell^-$ and $(g - 2)_\mu$ anomalies via loop contributions involving with new scalars and fermions. For this purpose, we first write down the most general Lagrangian which can generate the desired effects and then calculate the generic expressions for all relevant $b \rightarrow s$ Wilson coefficients. Here we extend previous analysis by allowing that the new particles can also couple to right-handed Standard Model (SM) fermions as preferred by recent $b \rightarrow s\ell^+\ell^-$ data and the anomalous magnetic moment of the muon.

In the second part of this article we illustrate this generic approach for a UV complete model in which we supplement the Standard Model by a 4th generation of vector-like fermions and a real scalar field. This model allows one to coherently address the observed anomalies in $b \rightarrow s\ell^+\ell^-$ transitions and in a_μ without violating the bounds from other observables (in particular $B_s - \bar{B}_s$ mixing) or LHC searches. In fact, we find that our global fit to this model, after the recent experimental updates, is very good and prefers couplings to right-handed SM fermions, showing the importance of our generic setup and calculation performed in the first part of the article.

Contents

1	Introduction	2
2	Generic Setup and Wilson Coefficients	3
2.1	$b \rightarrow s\mu^+\mu^-$ and $b \rightarrow s\gamma$ Transitions	5
2.2	$b \rightarrow s\nu\bar{\nu}$	8
2.3	$\Delta B = \Delta S = 2$ Processes	9
2.4	$D_0 - \bar{D}_0$ Mixing	10
2.5	Anomalous Magnetic Moment of the Muon	11
2.6	Modified Z Couplings	11
3	Experimental Constraints on Wilson Coefficients	13
3.1	$b \rightarrow s$ Transitions	13
3.2	Neutral Meson Mixing	15
3.3	Anomalous Magnetic Moment of the Muon	16
3.4	Z Decays	16
4	4th Generation Model	16
4.1	Lagrangian	17
4.2	Wilson Coefficients	18
4.3	Phenomenology	21
5	Conclusions and Outlook	24
A	Fierz Identities	25
B	Loop Functions	26
C	Real Scalars and Majorana Fermions	28
C.1	$b \rightarrow s\mu^+\mu^-$	29
C.2	$B_s - \bar{B}_s$ mixing	29
D	Crossed Diagrams with Complex Scalars	31
E	Posterior Distributions	31

1 Introduction

While no particles beyond the ones of the Standard Model (SM) have been observed at the LHC (so far), $b \rightarrow s\ell^+\ell^-$ data show a coherent pattern of deviations from the SM predictions with a significance of more than $4\text{--}5\sigma$ [1–8]. Recently, results of Belle and LHCb presented at Moriond EW 2019 [9, 10] confirmed these tensions, even though the significance for the new physics (NP) hypothesis, compared to the SM, did not change notably¹. In fact, including these new measurements, global fits of the Wilson coefficients governing $b \rightarrow s\ell^+\ell^-$ transitions [12–17] still find that NP scenarios can describe data much better than the SM, even though the preferences between the different scenarios changed with respect to the previous experimental situation.

Concerning concrete NP models giving the desired pattern in the effective theory with a good fit to data, most analyses focused on scenarios in which the required NP effects are generated at tree-level, either by the exchange of Z' vector bosons [18–41] or via lepto-quarks [42–73]. Nonetheless, since the size of the NP contribution required to account for current data is of the order of 20% compared to the (loop and CKM suppressed) amplitude of the SM, also new loop effects can in principle suffice for an explanation.

In this context, box contributions of heavy new scalars and fermions² (also within multi Higgs doublet models with right-handed neutrinos [75–77]) have been shown to be a viable option [78–81]³. Furthermore, an explanation of the anomalies in $b \rightarrow s\ell^+\ell^-$ via loop effects allows for interesting connections to Dark Matter [86–92] and typically leads to correlated imprints on other observables like the anomalous magnetic moment of the muon (a_μ). However, the effect here is in most models too small since a quite large NP contribution is needed to account from the tantalizing tension between the measurement [93] and the SM prediction of around $3\text{--}4\sigma$. In fact, Ref. [79] found that it is challenging to account for Δa_μ with TeV scale masses and not too large couplings to muons with a minimal particle content. In general, it has been argued [94] that one needs new sources of electroweak symmetry breaking (EWSB) if one aims at a high scale explanation of the anomalous magnetic moment of the muon. In the context of adding new scalars and fermions to the SM this can be achieved for example by a fourth generation of vector-like leptons coupling to the SM Higgs [94–102].

¹Note that deviations from the SM predictions have been observed in $b \rightarrow c\tau\nu$ transitions as well [11]. However, since these tensions cannot be explained by loop effects, we do not discuss them in this article.

²Box contributions of new vectors and fermions were studied in the context of Z' models with vector-like quarks in Ref. [74].

³Alternatively, models with large couplings to right-handed top quarks can give the desired effect via a W -loop [82–84], as first shown in the EFT context in Ref. [85].

Therefore, we extend in this article the analysis of Ref. [79] to include the possibility of new sources of EW symmetry breaking within the NP sector. For this purpose, an extension of the field content with respect to the minimal one of Ref. [79] is necessary, i.e. more than three new fields need to be added to the SM particle content. In doing so, new couplings to right-handed quarks and leptons are introduced which do not only affect a_μ but also lead to different effects in $b \rightarrow s\mu^+\mu^-$ (i.e. lead to solutions other than the purely left-handed $C_9 = -C_{10}$ one obtained in Ref. [79]). In fact, while before Moriond 2019 scenarios with left-handed current were in general preferred, now including right-handed contributions (both in quark and leptonic sectors) can even give a better fit to data [12–14, 16, 17].

A UV complete example of such a setup with new scalars and fermions couplings to left- and right-handed SM fermions is a model with a vector-like 4th generation. With respect to Ref. [103, 104], also aiming at an explanation of the $b \rightarrow s\ell^+\ell^-$ anomalies, we add not only a 4th generation of leptons but also of quarks [105–108] to the SM. However, instead of adding a Z' boson we supplement the model by a neutral scalar to get the desired loop-contributions. Furthermore, one can forbid the dangerous mixing effect between the SM fermions and the new vector-like ones by assigning $U(1)$ charges to the new particles (resembling R-parity in the MSSM).

This article is organized as follows: In Sec. 2 we define our generic setup, in which new scalars and fermions couple to SM quarks and leptons via Yukawa-like interactions. There, we also provide completely general expressions for the formulae of the relevant Wilson coefficients. We review the corresponding observables together with the current experimental situation in Sec. 3. Our generic approach of Sec. 2 is then applied to a specific UV complete model in Sec. 4, which contains a vector-like fourth generation of fermions and a neutral scalar. We study the phenomenology of this model in detail before we conclude in Sec. 5.

2 Generic Setup and Wilson Coefficients

In this section we define our generic setup and calculate completely general 1-loop expressions for contributions to $b \rightarrow s$ processes and the anomalous magnetic moment of the muon.

As outlined in the introduction, in the spirit of Refs. [78, 79] we add to the SM particle content a NP sector with vector-like fermions Ψ_A and new scalars Φ_M such that $b \rightarrow s\mu^+\mu^-$ transitions can be generated via box diagrams, as depicted in Fig. 1. In this respect, we generalize the previous analysis of Ref. [79] by including in addition couplings of new particles to $SU(2)$ singlet SM fermions. Moreover, we do not impose limitations on

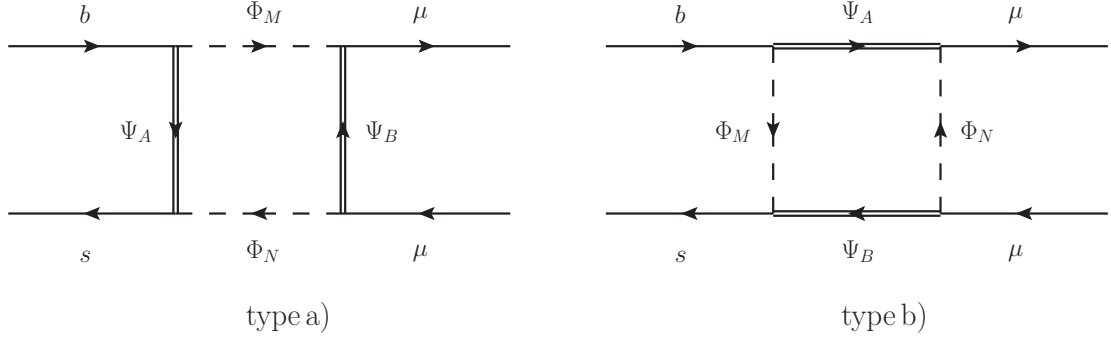


Figure 1. Box diagrams contributing to $b \rightarrow s\mu^+\mu^-$ transitions. The diagram on the left is generated in models in which the fermions couples only to SM quarks or only to SM leptons, which corresponds to type a). The diagram on the right refers to models with scalars connecting b to s and μ to μ , i.e. type b).

the number of fields added to the SM and allow for couplings of the new sector to the SM Higgs.

In order to generate box diagrams as the ones shown in Fig. 1 it is necessary that either the scalars $\Phi_{M,N}$ or the fermions $\Psi_{A,B}$ couple both to quarks and leptons, corresponding to case a) and b), respectively. This means that in diagrams of type a) the amplitudes (before using any Fierz identities) have the structure $(\bar{s}\Gamma b)(\bar{\mu}\Gamma\mu)$, while in type b) amplitudes of the form $(\bar{\mu}\Gamma b)(\bar{s}\Gamma\mu)$ are generated. Here, Γ denotes an arbitrary Dirac structure. Since semi-leptonic operators are commonly given in the form $(\bar{s}\Gamma b)(\bar{\mu}\Gamma\mu)$, Fierz identities must be used in case b) in order to transform the expressions to this standard basis. We give the relevant Fierz identities in Appendix A.

The Yukawa-like couplings of new scalars Φ_M and fermions Ψ_A to bottom/strange quarks and muons can be parameterized completely generically (below the EWSB scale) by the Lagrangian

$$\begin{aligned} \mathcal{L}_{\text{int}} = & \left[\bar{\Psi}_A \left(L_{AM}^b P_L b + L_{AM}^s P_L s + L_{AM}^\mu P_L \mu \right) \Phi_M \right. \\ & \left. + \bar{\Psi}_A \left(R_{AM}^b P_R b + R_{AM}^s P_R s + R_{AM}^\mu P_R \mu \right) \Phi_M \right] + \text{h.c.} \end{aligned} \quad (2.1)$$

Here Ψ_A and Φ_M have to be understood as generic lists containing in principle an arbitrary number of fields, meaning that A and M also include implicitly $SU(2)$ and color indices. Therefore, the couplings $L_{AM}^{s,b}$ and $R_{AM}^{s,b}$ are generic matrices in $(A-M)$ space with the restriction that $U(1)_{\text{EM}}$ and $SU(3)$ are respected⁴.

⁴Here we only consider coupling to muons in order to explain the anomalies in $b \rightarrow s\ell^+\ell^-$. The reason for this is that in our setup sizable couplings to electrons would in general generate effects in $\mu \rightarrow e\gamma$, which would contradict experimental bounds [109] by orders of magnitude.

This Lagrangian will not only affect $b \rightarrow s\mu^+\mu^-$ transitions but also unavoidably generate effects in $B_s - \bar{B}_s$ mixing, $b \rightarrow s\gamma$ decays, the anomalous magnetic moment of the muon a_μ as well as Z couplings and decays to SM fermions. Furthermore, $b \rightarrow s\nu\bar{\nu}$ processes and $D_0 - \bar{D}_0$ mixing can give relevant constraints once $SU(2)$ invariance at the NP scale is imposed. Therefore, all these processes have to be taken into account in a complete phenomenological analysis. In order to perform such an analysis, the Wilson coefficients of the relevant effective Hamiltonian must be known. We will calculate them in the following subsections.

2.1 $b \rightarrow s\mu^+\mu^-$ and $b \rightarrow s\gamma$ Transitions

The dimension-6 operators governing $b \rightarrow s\mu^+\mu^-$ and $b \rightarrow s\gamma$ transitions are contained in the effective Hamiltonian:

$$\mathcal{H}_{\text{eff}}^{\ell\ell} = -\frac{4G_F}{\sqrt{2}} V_{tb} V_{ts}^* \sum_i \left(C_i(\mu) \mathcal{O}_i(\mu) + C'_i(\mu) \mathcal{O}'_i(\mu) \right) + \text{h.c.}, \quad (2.2)$$

where

$$\begin{aligned} \mathcal{O}_7 &= \frac{e}{16\pi^2} m_b \bar{s} \sigma^{\mu\nu} P_R b F_{\mu\nu}, & \mathcal{O}_8 &= \frac{g_s}{16\pi^2} m_b \bar{s}_\alpha \sigma^{\mu\nu} P_R T_{\alpha\beta}^a b_\beta G_{\mu\nu}^a, \\ \mathcal{O}_9 &= \frac{\alpha_{\text{EM}}}{4\pi} (\bar{s} \gamma_\mu P_L b) (\bar{\mu} \gamma^\mu \mu), & \mathcal{O}_{10} &= \frac{\alpha_{\text{EM}}}{4\pi} (\bar{s} \gamma_\mu P_L b) (\bar{\mu} \gamma^\mu \gamma_5 \mu), \\ \mathcal{O}_S &= \frac{\alpha_{\text{EM}}}{4\pi} (\bar{s} P_R b) (\bar{\mu} \mu), & \mathcal{O}_P &= \frac{\alpha_{\text{EM}}}{4\pi} (\bar{s} P_R b) (\bar{\mu} \gamma_5 \mu), \\ \mathcal{O}_T &= \frac{\alpha_{\text{EM}}}{4\pi} (\bar{s} \sigma_{\mu\nu} b) (\bar{\mu} \sigma^{\mu\nu} P_R \mu), \end{aligned} \quad (2.3)$$

with e being the electron charge, α_{EM} the fine structure constant and g_s the $SU(3)$ gauge coupling. The primed operators are obtained by interchanging L and R . NP contributions from box diagrams will generate effects in $C_{9,10}^{(\prime)}$, $C_{S,P}^{(\prime)}$ and $\mathcal{O}_T^{(\prime)}$, while on-shell photon (gluon) penguins generate $C_{7(8)}^{(\prime)}$ and $C_9^{(\prime)}$, and Z -penguins $C_{9,10}^{(\prime)}$.

The box diagrams in Fig. 1, result in the following Wilson coefficients (here and in the remainder of the section, an implicit sum over all NP particles, i.e. A, B, M, N , is understood):

$$\begin{aligned} C_9^{\text{box}, a)} &= -\mathcal{N} \frac{\chi L_{AN}^{s*} L_{AM}^b}{32\pi\alpha_{\text{EM}} m_{\Phi_M}^2} [L_{BM}^{\mu*} L_{BN}^\mu + R_{BM}^{\mu*} R_{BN}^\mu] F(x_{AM}, x_{BM}, x_{NM}), \\ C_9^{\text{box}, b)} &= -\mathcal{N} \frac{\chi L_{BM}^{s*} L_{AM}^b}{32\pi\alpha_{\text{EM}} m_{\Phi_M}^2} \left[L_{AN}^{\mu*} L_{BN}^\mu F(x_{AM}, x_{BM}, x_{NM}) \right. \\ &\quad \left. - R_{AN}^{\mu*} R_{BN}^\mu \frac{m_{\Psi_A} m_{\Psi_B}}{m_{\Phi_M}^2} G(x_{AM}, x_{BM}, x_{NM}) \right], \\ C_{10}^{\text{box}, a)} &= \mathcal{N} \frac{\chi L_{AN}^{s*} L_{AM}^b}{32\pi\alpha_{\text{EM}} m_{\Phi_M}^2} [L_{BM}^{\mu*} L_{BN}^\mu - R_{BM}^{\mu*} R_{BN}^\mu] F(x_{AM}, x_{BM}, x_{NM}), \end{aligned} \quad (2.4)$$

$SU(3)$	$b \rightarrow s\ell\bar{\ell}$ type a)				$b \rightarrow s\ell\bar{\ell}$ type b)				χ
	Ψ_A	Ψ_B	Φ_M	Φ_N	Ψ_A	Ψ_B	Φ_M	Φ_N	
I	3	1	1	1	1	1	$\bar{3}$	1	1
II	1	$\bar{3}$	$\bar{3}$	$\bar{3}$	3	3	1	3	1
III	3	8	8	8	8	8	$\bar{3}$	8	4/3
IV	8	$\bar{3}$	$\bar{3}$	$\bar{3}$	3	3	8	3	4/3
V	$\bar{3}$	3	3	3	$\bar{3}$	$\bar{3}$	3	$\bar{3}$	2

Table 1. Table of the possible $SU(3)$ representations that can give an effect in $b \rightarrow s\ell^+\ell^-$ or $b \rightarrow s\nu\nu$ transitions via box diagrams. χ denotes the resulting group factor appearing in Eqs. (2.4)-(2.8) which also enters in $b \rightarrow s\nu\nu$ transitions.

$$C_{10}^{\text{box}, b)} = \mathcal{N} \frac{\chi L_{BM}^{s*} L_{AM}^b}{32\pi\alpha_{\text{EM}} m_{\Phi_M}^2} \left[L_{AN}^{\mu*} L_{BN}^\mu F(x_{AM}, x_{BM}, x_{NM}) + R_{AN}^{\mu*} R_{BN}^\mu \frac{m_{\Psi_A} m_{\Psi_B}}{m_{\Phi_M}^2} G(x_{AM}, x_{BM}, x_{NM}) \right], \quad (2.5)$$

$$C_S^{\text{box}, a)} = -\mathcal{N} \frac{\chi L_{AN}^{s*} R_{AM}^b}{16\pi\alpha_{\text{EM}} m_{\Phi_M}^2} [R_{BM}^{\mu*} L_{BN}^\mu + L_{BM}^{\mu*} R_{BN}^\mu] \frac{m_{\Psi_A} m_{\Psi_B}}{m_{\Phi_M}^2} G(x_{AM}, x_{BM}, x_{NM}),$$

$$C_S^{\text{box}, b)} = \mathcal{N} \frac{\chi L_{BM}^{s*} R_{AM}^b}{16\pi\alpha_{\text{EM}} m_{\Phi_M}^2} \left[R_{AN}^{\mu*} L_{BN}^\mu F(x_{AM}, x_{BM}, x_{NM}) + L_{AN}^{\mu*} R_{BN}^\mu \frac{m_{\Psi_A} m_{\Psi_B}}{2m_{\Phi_M}^2} G(x_{AM}, x_{BM}, x_{NM}) \right], \quad (2.6)$$

$$C_P^{\text{box}, a)} = \mathcal{N} \frac{\chi L_{AN}^{s*} R_{AM}^b}{16\pi\alpha_{\text{EM}} m_{\Phi_M}^2} [R_{BM}^{\mu*} L_{BN}^\mu - L_{BM}^{\mu*} R_{BN}^\mu] \frac{m_{\Psi_A} m_{\Psi_B}}{m_{\Phi_M}^2} G(x_{AM}, x_{BM}, x_{NM}),$$

$$C_P^{\text{box}, b)} = -\mathcal{N} \frac{\chi L_{BM}^{s*} R_{AM}^b}{16\pi\alpha_{\text{EM}} m_{\Phi_M}^2} \left[R_{AN}^{\mu*} L_{BN}^\mu F(x_{AM}, x_{BM}, x_{NM}) - L_{AN}^{\mu*} R_{BN}^\mu \frac{m_{\Psi_A} m_{\Psi_B}}{2m_{\Phi_M}^2} G(x_{AM}, x_{BM}, x_{NM}) \right], \quad (2.7)$$

$$C_T^{\text{box}, b)} = -\mathcal{N} \frac{\chi L_{BM}^{s*} R_{AM}^b L_{AN}^{\mu*} R_{BN}^\mu}{16\pi\alpha_{\text{EM}} m_{\Phi_M}^2} \frac{m_{\Psi_A} m_{\Psi_B}}{m_{\Phi_M}^2} G(x_{AM}, x_{BM}, x_{NM}), \quad (2.8)$$

$$C_{9,S,T}^{\text{box}} = C_{9,S,T}^{\text{box}} (L \leftrightarrow R), \quad C_{10,P}^{\text{box}} = -C_{10,P}^{\text{box}} (L \leftrightarrow R), \quad (2.9)$$

where we have defined

$$x_{AM} \equiv (m_{\Psi_A}/m_{\Phi_M})^2, \quad x_{BM} \equiv (m_{\Psi_B}/m_{\Phi_M})^2, \quad x_{NM} \equiv (m_{\Phi_N}/m_{\Phi_M})^2, \quad (2.10)$$

and

$$\mathcal{N}^{-1} = \frac{4G_F}{\sqrt{2}} V_{tb} V_{ts}^*. \quad (2.11)$$

$SU(3)$	Ψ_A	Φ_M	χ_γ	χ_g	$\tilde{\chi}_g$
I	3	1	1	1	0
II	1	$\bar{3}$	1	0	1
III	3	8	4/3	-1/6	3/2
IV	8	$\bar{3}$	4/3	3/2	-1/6
V	$\bar{3}$	3	2	-1	1

Table 2. Table of the different $SU(3)$ representations that can give non-zero effects via photon- and gluon-penguin diagrams to $b \rightarrow s\mu^+\mu^-$ transitions. χ_γ denotes the resulting group factor for the former contribution, while χ_g and $\tilde{\chi}_g$ represent the resulting group factors for the latter.

In the equations above, the labels A , B , M and N denote the particle (in case of several representations) and also include $SU(2)$ components, while the sum over $SU(3)$ indices is encoded in the group factors χ . The dimensionless loop functions F and G are defined in Appendix B.

Such box contributions are only possible if both color and electric charge are conserved. While the Wilson coefficients of $b \rightarrow s\ell\ell$ operators are insensitive to the electric charge of the particle in the box, concerning $SU(3)$, the different possible representations of the new particles lead to distinct group factors χ in Eqs. (2.4)-(2.8). These group factors are different for type a) and b) and are given for all the possible representations in Tab. 1. Furthermore, crossed box diagrams can be constructed in some particular cases. We give the corresponding expressions for such in Appendix C.1 for the real scalar (or Majorana fermion) case and in Appendix D for the crossed diagrams arising with complex scalars.

On-shell photon penguins diagrams in Fig. 2 affect $C_7^{(\prime)}$ while off-shell ones enter $C_9^{\gamma(\prime)}$:

$$C_7 = \mathcal{N} \frac{\chi_\gamma L_{AM}^b}{2m_{\Phi_M}^2} \left[L_{AM}^{s*} \left(Q_{\Phi_M} \tilde{F}_7(x_{AM}) - Q_{\Psi_A} F_7(x_{AM}) \right) + R_{AM}^{s*} \frac{4m_{\Psi_A}}{m_b} \left(Q_{\Phi_M} \tilde{G}_7(x_{AM}) - Q_{\Psi_A} G_7(x_{AM}) \right) \right], \quad (2.12)$$

$$C_9^\gamma = \mathcal{N} \frac{\chi_\gamma L_{AM}^{s*} L_{AM}^b}{2m_{\Phi_M}^2} \left[Q_{\Phi_M} \tilde{F}_9(x_{AM}) - Q_{\Psi_A} \tilde{G}_9(x_{AM}) \right], \quad (2.13)$$

$$C_7' = C_7(L \leftrightarrow R), \quad C_9^{\gamma'} = C_9^\gamma(L \leftrightarrow R), \quad (2.14)$$

where m_b is the b quark mass. Q_{Φ_M} and Q_{Ψ_A} are the electric charges of the NP fields Φ_M and Ψ_A , respectively. The conservation of electric charge imposes that $Q_{\Phi_M} + Q_{\Psi_A} = Q_d \equiv -1/3$. The color factors χ_γ , which depend on the $SU(3)$ representations of the new particles in the loop, are given in Tab. 2. The loop functions are defined in Appendix B. Note that the terms proportional to \tilde{F}_7 , \tilde{G}_7 and \tilde{F}_9 in Eqs. (2.12)-(2.14) stem from the diagram where the photon couples to the scalar Φ_M , while the terms proportional to F_7 , G_7 and \tilde{G}_9 stem from the diagram where the photon couples to the fermion Ψ_A .

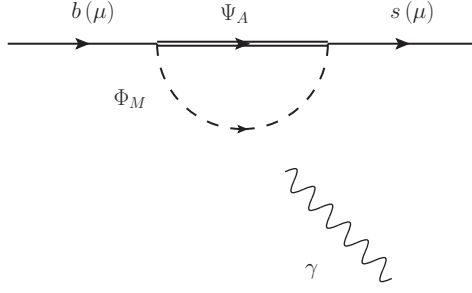


Figure 2. Photon-penguin diagrams contributing to $b \rightarrow s\gamma$ transitions and a_μ .

Similarly, the gluon-penguin generates

$$C_8 = \mathcal{N} \frac{L_{AM}^b}{2m_{\Phi_M}^2} \left[L_{AM}^{s*} \left(\chi_g \tilde{F}_7(x_{AM}) - \tilde{\chi}_g F_7(x_{AM}) \right) + R_{AM}^{s*} \frac{4m_{\Psi_A}}{m_b} \left(\chi_g \tilde{G}_7(x_{AM}) - \tilde{\chi}_g G_7(x_{AM}) \right) \right], \quad (2.15)$$

$$C'_8 = C_8 (L \leftrightarrow R), \quad (2.16)$$

where the color factors χ_g and $\tilde{\chi}_g$ for the different possible $SU(3)$ representations are given in Tab. 2.

The contribution of Z -penguins to $C_{9,10}^{(\prime)}$ is given in Sec. 2.6 together with a discussion of Z decays.

2.2 $b \rightarrow s\nu\bar{\nu}$

As stated at the beginning of this section, $b \rightarrow s\nu_\mu\bar{\nu}_\mu$ processes have to be taken into account once $SU(2)$ invariance at the NP scale is imposed. This implies that, in the generic description in Eq. (2.1), one has to replace the left-handed muon fields with neutrinos. The box diagrams generating $b \rightarrow s\nu_\mu\bar{\nu}_\mu$ are therefore obtained from Fig. 1 by replacing muons with neutrinos.

The effective Hamiltonian describing this process reads (following the conventions of Ref. [110])

$$\mathcal{H}_{\text{eff}}^{\nu_\mu} = -\frac{4G_F}{\sqrt{2}} V_{tb} V_{ts}^* (C_L \mathcal{O}_L + C_R \mathcal{O}_R) + \text{h.c.}, \quad (2.17)$$

where

$$\mathcal{O}_{L(R)} = \frac{\alpha_{\text{EM}}}{4\pi} [\bar{s} \gamma^\mu P_{L(R)} b] [\bar{\nu}_\mu \gamma_\mu (1 - \gamma^5) \nu_\mu]. \quad (2.18)$$

The resulting WCs are:

$$C_L^a) = -\mathcal{N} \frac{\chi L_{AN}^{s*} L_{AM}^b L_{BM}^{\mu*} L_{BN}^\mu}{32\pi \alpha_{\text{EM}} m_{\Phi_M}^2} F(x_{AM}, x_{BM}, x_{NM}),$$

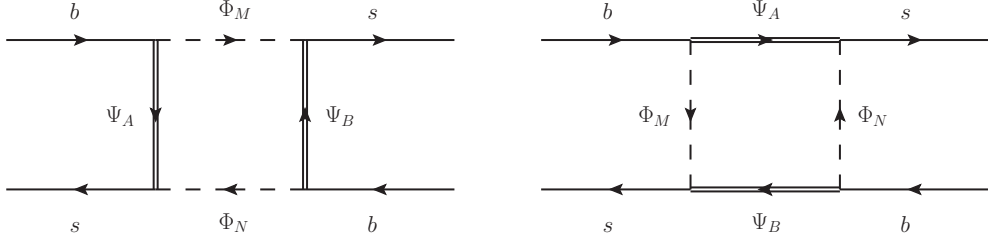


Figure 3. Box diagrams contributing to $B_s - \bar{B}_s$ mixing. Both diagrams arise independently of the nature of the mediator involved in $b \rightarrow s\mu^+\mu^-$ transitions.

$$C_L^b = \mathcal{N} \frac{\chi L_{BN}^{s*} L_{AM}^b L_{AN}^{\mu*} L_{BN}^\mu}{32\pi\alpha_{\text{EM}} m_{\Phi_M}^2} F(x_{AM}, x_{BM}, x_{NM}), \quad (2.19)$$

$$C_R^a = -\mathcal{N} \frac{\chi R_{AN}^{s*} R_{AM}^b L_{BM}^{\mu*} L_{BN}^\mu}{32\pi\alpha_{\text{EM}} m_{\Phi_M}^2} F(x_{AM}, x_{BM}, x_{NM}),$$

$$C_R^b = -\mathcal{N} \frac{\chi R_{BN}^{s*} R_{AM}^b L_{AN}^{\mu*} L_{BN}^\mu}{32\pi\alpha_{\text{EM}} m_{\Phi_M}^2} \frac{m_{\Psi_A} m_{\Psi_B}}{m_{\Phi_M}^2} G(x_{AM}, x_{BM}, x_{NM}), \quad (2.20)$$

where the normalization factor \mathcal{N} has been introduced in Eq. (2.11), and the loop functions $F(x, y, z)$ and $G(x, y, z)$ are defined in Appendix B. The colour factor χ is the same as for $b \rightarrow s\mu^+\mu^-$ transitions and is given in Tab. 1 for the different representations.

2.3 $\Delta B = \Delta S = 2$ Processes

The presence of $L_{AM}^{b,s}$ and $R_{AM}^{b,s}$ implies NP contributions to the $B_s - \bar{B}_s$ mixing which, using the conventions of Refs. [111, 112], is governed by

$$\mathcal{H}_{\text{eff}}^{B_s \bar{B}_s} = C_i \sum_{i=1}^5 \mathcal{O}_i + \tilde{C}_i \sum_{i=1}^3 \tilde{\mathcal{O}}_i + \text{h.c.}, \quad (2.21)$$

with

$$\begin{aligned} \mathcal{O}_1 &= (\bar{s}_\alpha \gamma^\mu P_L b_\alpha) (\bar{s}_\beta \gamma^\mu P_L b_\beta), & \tilde{\mathcal{O}}_1 &= (\bar{s}_\alpha \gamma^\mu P_R b_\alpha) (\bar{s}_\beta \gamma^\mu P_R b_\beta), \\ \mathcal{O}_2 &= (\bar{s}_\alpha P_L b_\alpha) (\bar{s}_\beta P_L b_\beta), & \tilde{\mathcal{O}}_2 &= (\bar{s}_\alpha P_R b_\alpha) (\bar{s}_\beta P_R b_\beta), \\ \mathcal{O}_3 &= (\bar{s}_\alpha P_L b_\beta) (\bar{s}_\beta P_L b_\alpha), & \tilde{\mathcal{O}}_3 &= (\bar{s}_\alpha P_R b_\beta) (\bar{s}_\beta P_R b_\alpha), \\ \mathcal{O}_4 &= (\bar{s}_\alpha P_L b_\alpha) (\bar{s}_\beta P_R b_\beta), \\ \mathcal{O}_5 &= (\bar{s}_\alpha P_L b_\beta) (\bar{s}_\beta P_R b_\alpha). \end{aligned} \quad (2.22)$$

The box diagrams contributing to these above operators are shown in Fig. 3. Using the Lagrangian from Eq. (2.1), one obtains the following results for the coefficients:

$$C_1 = (\chi_{BB} + \tilde{\chi}_{BB}) \frac{L_{AN}^{s*} L_{AM}^b L_{BM}^{s*} L_{BN}^b}{128\pi^2 m_{\Phi_M}^2} F(x_{AM}, x_{BM}, x_{NM}), \quad (2.23)$$

$SU(3)$	Ψ_A	Ψ_B	Φ_M	Φ_N	χ_{BB}	$\tilde{\chi}_{BB}$
I	3	3	1	1	1	0
II	1	1	$\bar{3}$	$\bar{3}$	0	1
III	3	3	8	8	1/36	7/12
IV	8	8	$\bar{3}$	$\bar{3}$	7/12	1/36
V	3	3	(1,8)	(8,1)	-1/6	1/2
VI	(1,8)	(8,1)	$\bar{3}$	$\bar{3}$	1/2	-1/6
VII	$\bar{3}$	$\bar{3}$	3	3	1	1

Table 3. Table of the different $SU(3)$ representations that can give a non-zero effect via box diagrams to $B_s - \bar{B}_s$ mixing. χ_{BB} and $\tilde{\chi}_{BB}$ denote the resulting group factors.

$$C_2 = \chi_{BB} \frac{R_{AN}^{s*} L_{AM}^b R_{BM}^{s*} L_{BN}^b}{64\pi^2 m_{\Phi_M}^2} \frac{m_{\Psi_A} m_{\Psi_B}}{m_{\Phi_M}^2} G(x_{AM}, x_{BM}, x_{NM}) , \quad (2.24)$$

$$C_3 = \tilde{\chi}_{BB} \frac{R_{AN}^{s*} L_{AM}^b R_{BM}^{s*} L_{BN}^b}{64\pi^2 m_{\Phi_M}^2} \frac{m_{\Psi_A} m_{\Psi_B}}{m_{\Phi_M}^2} G(x_{AM}, x_{BM}, x_{NM}) , \quad (2.25)$$

$$C_4 = \chi_{BB} \frac{R_{AN}^{s*} L_{AM}^b L_{BM}^{s*} R_{BN}^b}{32\pi^2 m_{\Phi_M}^2} \frac{m_{\Psi_A} m_{\Psi_B}}{m_{\Phi_M}^2} G(x_{AM}, x_{BM}, x_{NM}) \\ - \tilde{\chi}_{BB} \frac{R_{AN}^{s*} R_{AM}^b L_{BM}^{s*} L_{BN}^b}{32\pi^2 m_{\Phi_M}^2} F(x_{AM}, x_{BM}, x_{NM}) , \quad (2.26)$$

$$C_5 = \tilde{\chi}_{BB} \frac{R_{AN}^{s*} L_{AM}^b L_{BM}^{s*} R_{BN}^b}{32\pi^2 m_{\Phi_M}^2} \frac{m_{\Psi_A} m_{\Psi_B}}{m_{\Phi_M}^2} G(x_{AM}, x_{BM}, x_{NM}) \\ - \chi_{BB} \frac{R_{AN}^{s*} R_{AM}^b L_{BM}^{s*} L_{BN}^b}{32\pi^2 m_{\Phi_M}^2} F(x_{AM}, x_{BM}, x_{NM}) , \quad (2.27)$$

$$\tilde{C}_{1,2,3} = C_{1,2,3} (L \leftrightarrow R) . \quad (2.28)$$

The loop functions $F(x, y, z)$ and $G(x, y, z)$ are defined in Appendix B and the colour factors χ_{BB} and $\tilde{\chi}_{BB}$ are given in Tab. 3 for the different allowed representations. Again, in the presence of Majorana fermions or real scalars crossed diagrams can be constructed and the resulting expressions are given in Appendix C.2.

2.4 $D_0 - \bar{D}_0$ Mixing

NP contributions to the $D_0 - \bar{D}_0$ mixing can be obtained in complete generality (at the low scale) from Eqs. (2.23)-(2.28) by making the substitutions $s \rightarrow u$, $b \rightarrow c$, introducing couplings $L_{AM}^{u,c}$ and $R_{AM}^{u,c}$ of new scalars and fermions to up-quarks in straightforward extension of Eq. (2.1).

In the context a UV complete model, $SU(2)$ invariance imposes at the high scale that couplings to left-handed up-type quarks are related to the couplings to left-handed down-type quarks via CKM rotations. Therefore, working in the down-basis, the “minimal”

$SU(3)$	Ψ_A	Φ_M	χ_{a_μ}
I	1	1	1
II	$(3, \bar{3})$	$(3, \bar{3})$	3
III	8	8	8

Table 4. Table of the different $SU(3)$ representations that can give a non-zero effect to a_μ . χ_{a_μ} denotes the resulting group factor.

effect generated in $D_0 - \bar{D}_0$ is induced by the couplings

$$L_{AM}^u = V_{us}^* L_{AM}^s + V_{ub}^* L_{AM}^b, \quad L_{AM}^c = V_{cs}^* L_{AM}^s + V_{cb}^* L_{AM}^b. \quad (2.29)$$

2.5 Anomalous Magnetic Moment of the Muon

The anomalous magnetic moment of the muon ($a_\mu \equiv (g - 2)_\mu/2$) and its electric dipole moments (d_μ) we find from the diagrams in Fig. 2

$$\Delta a_\mu = \frac{\chi_{a_\mu} m_\mu^2}{8\pi^2 m_{\Phi_M}^2} \left[(L_{AM}^{\mu*} L_{AM}^\mu + R_{AM}^{\mu*} R_{AM}^\mu) (Q_{\Phi_M} \tilde{F}_7(x_{AM}) - Q_{\Psi_A} F_7(x_{AM})) \right. \\ \left. + (L_{AM}^{\mu*} R_{AM}^\mu + R_{AM}^{\mu*} L_{AM}^\mu) \frac{2m_{\Psi_A}}{m_\mu} (Q_{\Phi_M} \tilde{G}_7(x_{AM}) - Q_{\Psi_A} G_7(x_{AM})) \right], \quad (2.30)$$

$$d_\mu = \frac{\chi_{a_\mu} m_{\Psi_A}}{8\pi^2 m_{\Phi_M}^2} e (L_{AM}^{\mu*} R_{AM}^\mu - R_{AM}^{\mu*} L_{AM}^\mu) (Q_{\Phi_M} \tilde{G}_7(x_{AM}) - Q_{\Psi_A} G_7(x_{AM})), \quad (2.31)$$

where m_μ is the muon mass, χ_{a_μ} is the colour factor given in Table 4, and Q_{Φ_M} and Q_{Ψ_A} are the electric charges of the NP fields Φ_M and Ψ_A , respectively. Analogously to photon-penguin contributions to $b \rightarrow s$ transitions, the conservation of electric charge imposes that $Q_{\Phi_M} + Q_{\Psi_A} = Q_\mu \equiv -1$. Finally, the loop functions $F_7(x)$, $\tilde{F}_7(x)$, $G_7(x)$ and $\tilde{G}_7(x)$ are defined in Appendix B.

2.6 Modified Z Couplings

Here, we study the effects of our new particles on modified Z couplings, i.e. on $Z\bar{\mu}\mu$, $Z\bar{b}b$, $Z\bar{s}s$ and $Z\bar{b}b$ couplings, both for off- and on-shell Z bosons⁵. We define the form-factors governing $Z\bar{f}f$ interactions as [114]

$$- \frac{g_2}{c_W} \bar{f}' \gamma^\mu \left[g_L^{f'f}(q^2) P_L + g_R^{f'f}(q^2) P_R \right] f Z_\mu + \text{h.c.}, \quad (2.32)$$

where $f = \{b, s, \mu\}$, g_2 is the $SU(2)$ gauge coupling, θ_W the Weinberg angle and q is the Z momentum. Moreover,

$$g_{L(R)}^{f'f}(q^2) = g_{fL}^{\text{SM}} \delta_{f'f} + \Delta g_{L(R)}^{f'f}(q^2) \quad (2.33)$$

⁵Expressions for Z couplings in generic gauge theories can be found in Ref. [113].

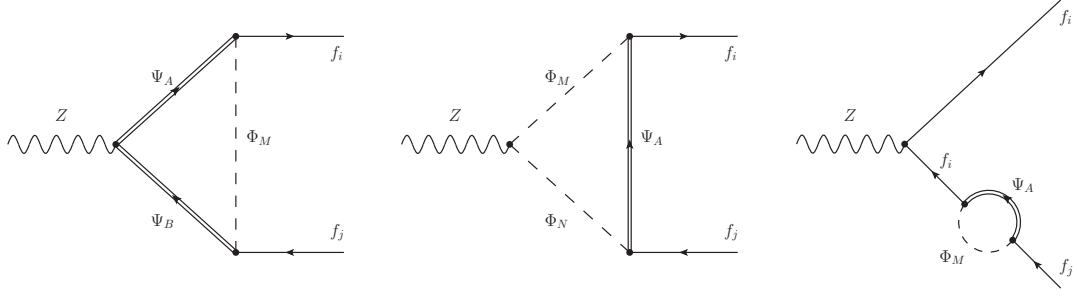


Figure 4. Feynman diagrams modifying the $Z \bar{f}_i f_j$ vertex with $f_i = s, b, \mu$.

with $g_{f_L}^{\text{SM}} = (T_3^f - Q_f s_W^2)$ and $g_{f_R}^{\text{SM}} = -Q_f s_W^2$ being the Z couplings to SM fermions at tree-level. The relevant Feynman diagrams are shown in Fig. 4. We write the coupling of the Z boson to the new scalars and fermions as

$$\mathcal{L}^Z = -\frac{g_2}{c_W} Z_\mu \left(\bar{\Psi}_A \gamma^\mu \left[g_{AB}^{\Psi,L} P_L + g_{AB}^{\Psi,R} P_R \right] \Psi_B + g_{MN}^\Phi \Phi_M^\dagger i \overleftrightarrow{\partial}^\mu \Phi_N \right) + \text{h.c.}, \quad (2.34)$$

where we have introduced the notation $a \overleftrightarrow{\partial}^\mu b = a(\partial^\mu b) - (\partial^\mu a)b$, and with generic couplings $g_{AB}^{\Psi,L,R}$ and g_{MN}^Φ which can only be determined in a UV complete model in which also the couplings of the new particles to the SM Higgs are known. Using the generic Lagrangian from Eq. (2.1), one obtains the following results for the coefficients

$$\begin{aligned} \Delta g_L^{f'f}(q^2) = & \frac{\chi_Z L_{BN}^{f'} L_{AM}^{f*}}{32\pi^2} \\ & \left[2 g_{AB}^{\Psi,L} \delta_{MN} \frac{m_{\Psi_A} m_{\Psi_B}}{m_{\Phi_M}^2} G_Z(x_{AM}, x_{BM}) - g_{AB}^{\Psi,R} \delta_{MN} F_Z(x_{AM}, x_{BM}, m_{\Phi_M}) \right. \\ & + g_{MN}^\Phi \delta_{AB} H_Z(x_{AM}, x_{AN}, m_{\Psi_A}) - \frac{1}{2} (g_{f_L}^{\text{SM}} + g_{f'_L}^{\text{SM}}) \delta_{AB} \delta_{MN} I_Z(x_{AM}, m_{\Phi_M}) \\ & + q^2 \left(g_{AB}^{\Psi,L} \delta_{MN} \frac{m_{\Psi_A} m_{\Psi_B}}{m_{\Phi_M}^4} \tilde{G}_Z(x_{AM}, x_{BM}) - \frac{2}{3} \frac{g_{AB}^{\Psi,R} \delta_{MN}}{m_{\Phi_M}^2} \tilde{F}_Z(x_{AM}, x_{BM}) \right. \\ & \left. \left. - \frac{1}{3} \frac{g_{MN}^\Phi \delta_{AB}}{m_{\Psi_A}^2} \tilde{H}_Z(x_{AM}, x_{AN}) \right) \right], \quad (2.35) \end{aligned}$$

$$\Delta g_R^{f'f}(q^2) = \Delta g_L^{f'f}(q^2) (L \leftrightarrow R), \quad (2.36)$$

where the loop functions are defined in Appendix B, and the colour factor $\chi_Z = \chi_\gamma$ for $f, f' = b, s$ (see Table 2) and $\chi_Z = \chi_{a_\mu}$ (see Table 4) for $f = \mu$. Here we have set the masses and momenta of the external fermions to 0 and expanded up to first order in q^2 over the NP scale. If one is considering data from Z decays, Eq. (2.35) has to be evaluated to $q^2 = m_Z^2$ while for processes with an off-shell Z (like $b \rightarrow s \ell^+ \ell^-$) one has to set $q^2 = 0$.

Note that in the absence of EW symmetry breaking in the NP sector, the contribution of the self-energies cancel the one of the genuine vertex correction and Eq. (2.35) vanishes

for $q^2 = 0$. Therefore, as noted above, $g_{AB}^{\Psi,L}$, $g_{AB}^{\Psi,R}$ and g_{MN}^Φ are only meaningful after EWSB and it is not possible to relate them purely to $SU(2) \times U(1)$ quantum numbers. In a specific UV model with a known pattern of EWSB, rotation matrices can be used to relate the couplings before and after the breaking. Consequently, the cancellation of UV divergences (present in some of the loop functions in Eq. (2.35)) is only manifest after summation over $SU(2)$ indices, due to a GIM-like cancellation originating from the unitarity of the rotation matrices. We will give a concrete example of this in Sec. 4.

The form-factors in Eq. (2.32) includes $Z\bar{s}b$ couplings generating contributions to $C_{9,10}^{(\prime)}$

$$C_9^{(\prime)Z} = \mathcal{N} \frac{\pi g^2}{\alpha_{\text{EM}} c_W^2 m_Z^2} g_{L(R)}^{sb}(q^2 = 0) (1 - 4s_W^2) , \quad (2.37)$$

$$C_{10}^{(\prime)Z} = -\mathcal{N} \frac{\pi g^2}{\alpha_{\text{EM}} c_W^2 m_Z^2} g_{L(R)}^{sb}(q^2 = 0) . \quad (2.38)$$

Note that these contributions are lepton flavour universal and therefore cannot account for R_K and R_{K^*} . However, a mixture of lepton flavour universal and violating contributions is phenomenologically interesting [115], especially in the light of the recent Belle and LHCb measurements [12, 15]. In a similar fashion, $Z\bar{s}b$ couplings will also generate the following contributions to $b \rightarrow s\nu\bar{\nu}$ contained in $C_{L(R)}$

$$C_{L(R)}^Z = -\mathcal{N} \frac{\pi g^2}{\alpha_{\text{EM}} c_W^2 m_Z^2} g_{L(R)}^{sb}(q^2 = 0) . \quad (2.39)$$

Finally, if $SU(2)$ invariance at the NP scale is imposed, the new scalars and fermions couple also the neutrinos. Hence, contributions to $Z \rightarrow \nu\bar{\nu}$ and $W \rightarrow \mu\bar{\nu}$ will arise as well. Concerning $Z \rightarrow \nu\bar{\nu}$, $g_{\nu_L}(q^2 = m_Z^2)$ can be straightforwardly extracted from Eq. (2.35) by appropriate replacements and the same is true concerning $W\mu\bar{\nu}$ couplings.

3 Experimental Constraints on Wilson Coefficients

In this section we review the experimental situation and the resulting constraints on the Wilson coefficients calculated in the previous section.

3.1 $b \rightarrow s$ Transitions

The semileptonic operators $\mathcal{O}_{9,10}^{(\prime)}$, $\mathcal{O}_{S,P}^{(\prime)}$ and $\mathcal{O}_T^{(\prime)}$, together with magnetic operators $\mathcal{O}_7^{(\prime)}$, contribute to a plethora of $b \rightarrow s\ell^+\ell^-$ observables. The corresponding measurements include total branching ratios of $B_s \rightarrow \ell^+\ell^-$ [11], of the exclusive decays $B \rightarrow K^*\gamma$ [11], $B \rightarrow \phi\gamma$ [116], the inclusive decay $B \rightarrow X_s\gamma$ [11], the angular analyses of $B \rightarrow K^{(*)}\ell^+\ell^-$ [117–123] (proposed in Refs. [124–126]) and $B_s \rightarrow \phi\ell^+\ell^-$ [127], and also the ratios R_K [9] and R_{K^*} [10, 128] measuring lepton flavour universality violation.

First of all, the contributions of scalar operators are helicity-enhanced in the $B_s \rightarrow \mu^+ \mu^-$ branching ratio with respect to the O_{10} contribution of the SM. This results in the bound [129]

$$\frac{\mathcal{B}^{\text{exp}}(B_s \rightarrow \mu^+ \mu^-)}{\mathcal{B}^{\text{SM}}(B_s \rightarrow \mu^+ \mu^-)} - 1 = \left| 1 + \frac{C_{10} - C'_{10}}{C_{10}^{\text{SM}}} + \frac{m_{B_s}^2}{2m_\mu(m_b + m_s)} \frac{C_P - C'_P}{C_{10}^{\text{SM}}} \right|^2 + \frac{m_{B_s}^2(m_{B_s}^2 - 4m_\mu^2)}{4m_\mu^2(m_b + m_s)^2} \left| \frac{C_S - C'_S}{C_{10}^{\text{SM}}} \right|^2 - 1 = -0.13 \pm 0.20, \quad (3.1)$$

which excludes sizable contributions to scalar operators (unless there is a purely scalar quark current) and leads to

$$|C_{S,P}^{(\prime)}| \lesssim 0.03 \quad (2\sigma), \quad (3.2)$$

from the updated one-parameter fit of Ref. [130]. Therefore, we neglect the effects of scalar operators in semi-leptonic B since they anyway cannot explain the corresponding anomalies.

Moreover, the inclusive $b \rightarrow s\gamma$ decay strongly constrains the magnetic operators. From [131, 132], in the limit of vanishing $C'_{7,8}$ ⁶, we have

$$\frac{\mathcal{B}^{\text{exp}}(b \rightarrow s\gamma)}{\mathcal{B}^{\text{SM}}(b \rightarrow s\gamma)} - 1 = -2.87 [C_7 + 0.19 C_8] = (-0.7 \pm 8.2) \times 10^{-2}, \quad (3.3)$$

leading to

$$|C_7 + 0.19 C_8| \lesssim 0.06 \quad (2\sigma). \quad (3.4)$$

Here, we used $C_{7,8}$ at a matching scale of 1 TeV as input. Again, these constraints are so stringent that the effect of $C_{7,8}$ on the flavour anomalies can be mostly neglected.

On the other hand, vector operators can explain the $b \rightarrow s\ell^+\ell^-$ anomalies. We therefore refer to global fits to constrain $C_{9,10}^{(\prime)}$, where all the relevant observables have been taken into account [1–8]. The results of the most recent fits find at the 2σ level

$$\begin{aligned} -1.48 \leq C_9 \leq -0.71, & \quad -0.12 \leq C_{10} \leq 0.61, \\ -0.56 \leq C'_9 \leq 1.14, & \quad -0.57 \leq C'_{10} \leq 0.34, \end{aligned}$$

according to Ref. [12] (which is compatible with Refs. [13, 14, 16, 17]).

As explained in Sec. 2.2, $SU(2)$ invariance implies the presence of contributions to $B \rightarrow K^{(*)}\nu\bar{\nu}$ decays as well. Since there is no experimental way to distinguish different neutrino

⁶Note that $C'_{7,8}$ are less constrained since they do not interfere with the SM. For a more detailed analysis including primed operators see e.g. Ref. [133].

flavours in these decays, one measures the total branching ratio which we normalize to its SM prediction [110]:

$$R_{K^{(*)}}^{\nu\bar{\nu}} = \frac{\mathcal{B}^{\text{exp}}(B \rightarrow K^{(*)}\nu\bar{\nu})}{\mathcal{B}^{\text{SM}}(B \rightarrow K^{(*)}\nu\bar{\nu})} = \frac{2(C_L^{\text{SM}})^2 + (C_L^{\text{SM}} + C_L)^2 - \kappa (C_L^{\text{SM}} + C_L)C_R + C_R^2}{3(C_L^{\text{SM}})^2}. \quad (3.5)$$

In the case of a K in the final state one has $\kappa \equiv -2$, while for the K^* one gets $\kappa = 1.34(4)$ [110]. The current experimental limits at 90% C.L. are [134]

$$R_K^{\nu\bar{\nu}} < 3.9, \quad R_{K^*}^{\nu\bar{\nu}} < 2.7. \quad (3.6)$$

3.2 Neutral Meson Mixing

The experimental constraint on the Wilson coefficients in Eqs. (2.23)-(2.28) comes from the mass difference ΔM_s of neutral B_s mesons, see e.g. Ref. [111] (in the case of real Wilson coefficients). To compare our results with experiments we use

$$\begin{aligned} \frac{\Delta M_s^{\text{exp}}}{\Delta M_s^{\text{SM}}} &= \left| 1 + \sum_{i,j=1}^3 R_i(\mu_b) \frac{\eta_{ij}(\mu_b, \mu_H)}{C_1^{\text{SM}}(\mu_b)} (C_j + \tilde{C}_j) + \sum_{i,j=4}^5 R_i(\mu_b) \frac{\eta_{ij}(\mu_b, \mu_H)}{C_1^{\text{SM}}(\mu_b)} C_j \right| \\ &= \left| 1 + \frac{0.8(C_1 + \tilde{C}_1) - 1.9(C_2 + \tilde{C}_2) + 0.5(C_3 + \tilde{C}_3) + 5.2C_4 + 1.9C_5}{C_1^{\text{SM}}(\mu_b)} \right|, \end{aligned} \quad (3.7)$$

where $R_i(\mu_b)$ is related to the matrix element of the operators Q_i in Eq. (2.22) at the scale μ_b by the relation

$$R_i(\mu_b) = \frac{\langle \bar{B}_s | Q_i(\mu_b) | B_s \rangle}{\langle \bar{B}_s | Q_1(\mu_b) | B_s \rangle}. \quad (3.8)$$

The coefficients C_i and \tilde{C}_i are the ones in Eqs. (2.23)-(2.28), computed at the NP scale μ_H . The matrix in operator space $\eta_{ij}(\mu_b, \mu_H)$ encodes the QCD evolution from the high scale μ_H to μ_b , which we calculated numerically for a reference scale $\mu_H = 1$ TeV [135]. The matrix elements in Eqs. (3.7)-(3.8) have been computed by a $N_f = 2 + 1$ lattice simulation [136], which found values consistent with the $N_f = 2$ calculation [137] and recent sum rules results [138]. It is worth mentioning that FLAG-2019 [139] only provides a lattice average for $\langle \bar{B}_s | Q_1(\mu_b) | B_s \rangle$, which is however dominated by the $N_f = 2 + 1$ results from Ref. [136]. Therefore, we decided to employ the results from Ref. [136] in Eqs. (3.7)-(3.8). The SM value for the Wilson coefficient is $C_1^{\text{SM}}(\mu_b) = \frac{G_F^2 M_W^2}{4\pi^2} \lambda_t^2 \eta_{11}(\mu_b, m_t) S_0(x_t) \simeq 7.2 \times 10^{-11} \text{ GeV}^{-2}$.

The experimental constraint therefore reads [140]

$$R_{\Delta M_s} = \frac{\Delta M_s^{\text{exp}}}{\Delta M_s^{\text{SM}}} - 1 = -0.09 \pm 0.08, \quad (3.9)$$

computed with the values from Ref. [136] for $\langle \bar{B}_s | Q_1(\mu_b) | B_s \rangle$. This value shows a slight tension with the SM as first outlined in Refs. [141, 142]. The tension would be reduced

if one considered the results for the matrix element from Ref. [138]: however, in this case one should rely on a separate computation for the decay constant, while in Ref. [136] both quantities are computed together.

Analogously to the B_s system, $D_0 - \bar{D}_0$ mixing is constrained by the mass difference of neutral D_0 mesons [140]:

$$\Delta M_{D_0}^{\text{exp}} = (0.63_{-0.29}^{+0.27}) \times 10^{-11} \text{MeV}. \quad (3.10)$$

Unfortunately, a precise SM prediction is still lacking in this sector but one can constrain the NP contribution by assuming that not more than the total mass difference is generated by it.

3.3 Anomalous Magnetic Moment of the Muon

From the experimental side, this quantity has been already measured quite precisely [93], but further improvements by experiments at Fermilab [143] and J-PARC [144] (see also [145]) are expected in the future. On the theory side, the SM prediction has been improved continuously [146–169]. The current tension between the two determinations accounts to

$$\Delta a_\mu = a_\mu^{\text{exp}} - a_\mu^{\text{SM}} \sim 270(85) \times 10^{-11}. \quad (3.11)$$

3.4 Z Decays

The main experimental measurements of Z couplings have been performed at LEP [170] (at the Z pole). We extract from the model independent analysis of Ref. [171] the values for the NP contributions ⁷

$$\begin{aligned} \Delta g_{\mu_L}(m_Z^2) &= -(0.1 \pm 1.1) \times 10^{-3}, & \Delta g_{\mu_R}(m_Z^2) &= (0.0 \pm 1.3) \times 10^{-3}, \\ \Delta g_{b_L}(m_Z^2) &= -(0.33 \pm 0.16) \times 10^{-2}, & \Delta g_{b_R}(m_Z^2) &= -(2.30 \pm 0.82) \times 10^{-3}, \\ \Delta g_{\nu_L}(m_Z^2) &= (0.40 \pm 0.21) \times 10^{-2}, & & \end{aligned} \quad (3.12)$$

neglecting cancellations and correlations.

4 4th Generation Model

In this section we propose a model with a vector-like 4th generation of fermions and a new complex scalar. This will also allow us to apply and illustrate the generic findings of the previous section to a UV complete model and study the effects in $b \rightarrow s\ell^+\ell^-$ data and a_μ .

⁷ Z couplings in Ref. [171] are defined with opposite sign with respect to our conventions [114].

4.1 Lagrangian

The Lagrangian for our 4th generation model is obtained from the SM one by adding a 4th vector-like generation [103, 104] and a neutral scalar

$$\begin{aligned}
L^{4\text{th}} = & \sum_i \left(\Gamma_{q_i}^L \bar{\Psi}_q P_L q_i + \Gamma_{\ell_i}^L \bar{\Psi}_\ell P_L \ell_i + \Gamma_{u_i}^R \bar{\Psi}_u P_R u_i + \Gamma_{d_i}^R \bar{\Psi}_d P_R d_i + \Gamma_{e_i}^R \bar{\Psi}_e P_R e_i \right) \Phi + \text{h.c.} \\
& + \sum_{C=L,R} \left(\lambda_C^U \bar{\Psi}_q P_C \tilde{h} \Psi_u + \lambda_C^D \bar{\Psi}_q P_C h \Psi_d + \lambda_C^E \bar{\Psi}_\ell P_C h \Psi_e \right) + \text{h.c.} \\
& + \sum_{F=q,\ell,u,d,e} M_F \bar{\Psi}_F \Psi_F + \kappa h^\dagger h \Phi^\dagger \Phi + m_\Phi^2 \Phi^\dagger \Phi,
\end{aligned} \tag{4.1}$$

where i is a family index and h the SM Higgs doublet. The charge assignments for the new vector-like fermions $\Psi = \Psi_L + \Psi_R$ with $P_{L,R} \Psi = \Psi_{L,R}$ and the new scalar Φ are

	$SU(3)$	$SU(2)$	$U(1)$	$U'(1)$
Ψ_q	3	2	1/6	Z
Ψ_u	3	1	2/3	Z
Ψ_d	3	1	-1/3	Z
Ψ_ℓ	1	2	-1/2	Z
Ψ_e	1	1	-1	Z
Φ	1	1	0	$-Z$

(4.2)

The SM fermions have the same $SU(3) \times SU(2) \times U(1)$ charge assignments of the relative NP fermion partner, and the higgs transforms as a (1, 2, 1/2). Here we assigned to the new particles also charges under a new $U(1)$ group in order to forbid mixing with the SM particles, giving a similar effect as R-parity in the MSSM⁸. From Table 4.2 we see that concerning $SU(3)$ we are dealing with cases I of our generic analysis in Tables 1-4. In particular, concerning $b \rightarrow s\mu^+\mu^-$, this model would generate diagrams of type a) in Fig. 1.

After EWSB, mass matrices for the new fermions are generated

$$\begin{aligned}
L_{\text{mass}}^{4\text{th}} = & \begin{pmatrix} \bar{\Psi}_{q,1} \\ \bar{\Psi}_u \end{pmatrix}^T \mathbf{M}_U P_L \begin{pmatrix} \Psi_{q,1} \\ \Psi_u \end{pmatrix} + \begin{pmatrix} \bar{\Psi}_{q,2} \\ \bar{\Psi}_d \end{pmatrix}^T \mathbf{M}_D P_L \begin{pmatrix} \Psi_{q,2} \\ \Psi_d \end{pmatrix} \\
& + \begin{pmatrix} \bar{\Psi}_{\ell,2} \\ \bar{\Psi}_e \end{pmatrix}^T \mathbf{M}_E P_L \begin{pmatrix} \Psi_{\ell,2} \\ \Psi_e \end{pmatrix} + \text{h.c.},
\end{aligned} \tag{4.3}$$

where $\mathbf{M}_{U,D,E}$ are non-diagonal mass matrices

$$\mathbf{M}_{D(U)} = \begin{pmatrix} M_q & \sqrt{2}v\lambda_R^{D(U)} \\ \sqrt{2}v\lambda_L^{D(U)*} & M_{d(u)} \end{pmatrix}, \quad \mathbf{M}_E = \begin{pmatrix} M_\ell & \sqrt{2}v\lambda_R^E \\ \sqrt{2}v\lambda_L^{E*} & M_e \end{pmatrix}. \tag{4.4}$$

⁸We did not assume a Z_2 symmetry because this would allow the scalar Φ to be real and lead to crossed boxes in $b \rightarrow s\ell^+\ell^-$, canceling the desired effect there.

Here the subscripts 1 and 2 denote the $SU(2)$ component of the doublet. We diagonalize these mass matrices by performing the field redefinitions

$$\begin{aligned}
P_L \begin{pmatrix} \Psi_{q,1} \\ \Psi_u \end{pmatrix}_I &\rightarrow W_{IJ}^{U_L} \Psi_J^{U_L}, & P_L \begin{pmatrix} \Psi_{q,2} \\ \Psi_d \end{pmatrix}_I &\rightarrow W_{IJ}^{D_L} \Psi_J^{D_L}, & + & L \rightarrow R \\
P_L \Psi_{L,1} &\rightarrow \Psi^{N_L}, & P_L \begin{pmatrix} \Psi_{\ell,2} \\ \Psi_e \end{pmatrix}_I &\rightarrow W_{IJ}^{E_L} \Psi_J^{E_L}, & + & L \rightarrow R
\end{aligned} \quad (4.5)$$

leading to

$$(W^{F_L \dagger} \mathbf{M}_F W^{F_R})_{IJ} = m_{F_I} \delta_{IJ}, \quad \text{with } F = U, D, E. \quad (4.6)$$

Therefore, after EWSB we have the mass eigenstates $\Psi_I^{U_{L,R}}$, $\Psi_I^{D_{L,R}}$, $\Psi_I^{E_{L,R}}$ and $\Psi^{N_{L,R}}$, with $I = \{1, 2\}$. In particular, $\Psi_I^{U_{L,R}}$ and $\Psi_I^{D_{L,R}}$ ($\Psi_I^{E_{L,R}}$ and $\Psi^{N_{L,R}}$) are $SU(3)$ triplets (singlets) with the same electric charges as up-type and down-type quarks (charged-leptons and neutrinos), respectively.

The rotations introduced at Eq. (4.5) lead to the following Lagrangian for the interactions in the broken phase

$$\begin{aligned}
L_{\text{int}}^{4\text{th}} &= \left(L_I^{d_i} \bar{\Psi}_I^D P_L d_i + L_I^{e_i} \bar{\Psi}_I^E P_L e_i + R_I^{d_i} \bar{\Psi}_I^D P_R d_i + R_I^{e_i} \bar{\Psi}_I^E P_R e_i \right) \Phi \\
&+ \left(L_I^{u_i} \bar{\Psi}_I^U P_L u_i + L^{\nu_i} \bar{\Psi}^N P_L \nu_i + R_I^{u_i} \bar{\Psi}_I^U P_R u_i \right) \Phi + \text{h.c.}
\end{aligned} \quad (4.7)$$

which resembles Eq. (2.1) for the special case of our 4th generation model. Thus identify

$$\begin{aligned}
L_I^{d_i} &= \Gamma_{q_i}^L W_{1I}^{D_R*}, & L_I^{e_i} &= \Gamma_{\ell_i}^L W_{1I}^{E_R*}, & L_I^{u_i} &= \Gamma_{q_j}^L V_{ij}^* W_{1I}^{U_R*}, & L^{\nu_i} &= \Gamma_{\ell_i}^L, \\
R_I^{d_i} &= \Gamma_{d_i}^R W_{2I}^{D_L*}, & R_I^{e_i} &= \Gamma_{e_i}^R W_{2I}^{E_L*}, & R_I^{u_i} &= \Gamma_{u_i}^R W_{2I}^{U_L*}.
\end{aligned} \quad (4.8)$$

Here we worked in the down-basis for the SM quarks which means that CKM matrices V_{ij} appear in vertices involving up-type quarks. The first two columns of the above Lagrangian involves couplings with down-type quarks and charged leptons and can be directly matched on the Lagrangian in Eq. (2.1) for the case of only one scalar, i.e. $\Phi_M \equiv \Phi$ and $\Psi_A \equiv \{\Psi_I^D, \Psi_I^E\}$. The presence of $L_I^{u_i}$ (L^{ν_i}) resembles the fact, mentioned in Sec. 2, that left-handed couplings to down-quarks (leptons) lead via $SU(2)$ to couplings to left-handed up-quarks (neutrinos). In addition couplings to right-handed up-quarks $R_I^{u_i}$ appear in our model which are however not relevant for our phenomenology.

4.2 Wilson Coefficients

With these conventions we can now easily derive the Wilson coefficients within our model which can be directly obtained from the results of Sec. 2. In order to simplify the expressions, we will assume $M_Q = M_d \equiv m_D$ and $M_L = M_e \equiv m_E$ and only take into account couplings to b , s and μ in Eq. (4.1):

$$\{\Gamma_s^L, \Gamma_b^L, \Gamma_\mu^L, \Gamma_s^R, \Gamma_b^R, \Gamma_\mu^R\}, \quad (4.9)$$

Concerning $SU(2)$ breaking effects the couplings $\lambda_{L,R}^D$ and $\lambda_{L,R}^E$ related to the down and charged leptons sector, respectively, can be relevant. However, concerning $\lambda_{L,R}^D$ recall that from Section 3.1 that experimental data suggests very small values for $C_{S,P}$ and $C_{7,8}$. In our model this can be achieved by assuming $\lambda_{L,R}^D = 0$ ⁹. In this limit the mass matrix \mathbf{M}^D in Eq. (4.4) is diagonal and the corresponding rotation matrices $W^{D_{R(L)}}$ in Eq. (4.6) are equal to the identity, which implies

$$C_{S,P} \propto L_A^{s*} R_A^b \propto W_{1A}^{D_R} W_{2A}^{D_L*} = \delta_{1A} \delta_{2A} = 0. \quad (4.10)$$

With this setup, we obtain the following non-vanishing couplings in the quark sector of the Lagrangian in Eq. (4.7):

$$\begin{aligned} L_1^s &= \Gamma_s^L, & L_1^b &= \Gamma_b^L, & R_2^s &= \Gamma_s^R, & R_2^b &= \Gamma_b^R, \\ L_1^u &= V_{us}^* \Gamma_s^L + V_{ub}^* \Gamma_b^L, & L_1^c &= V_{cs}^* \Gamma_s^L + V_{cb}^* \Gamma_b^L. \end{aligned} \quad (4.11)$$

with

$$\Gamma^L \equiv L_1^b L_1^{s*}, \quad \Gamma^R \equiv R_2^b R_2^{s*}, \quad x_{D(E)} \equiv \frac{m_{D(E)}^2}{m_\Phi^2}. \quad (4.12)$$

The expressions of Wilson coefficients for $b \rightarrow s$ processes simplify to:

- $b \rightarrow s\mu^+\mu^-$ and $b \rightarrow s\gamma$ (see Eqs. (2.4)-(2.16))

$$C_9^{\text{box}} = -\mathcal{N} \frac{\Gamma^L}{32\pi\alpha_{\text{EM}}m_\Phi^2} (|\Gamma_\mu^L|^2 + |\Gamma_\mu^R|^2) F(x_D, x_E), \quad (4.13)$$

$$C_{10}^{\text{box}} = \mathcal{N} \frac{\Gamma^L}{32\pi\alpha_{\text{EM}}m_\Phi^2} (|\Gamma_\mu^L|^2 - |\Gamma_\mu^R|^2) F(x_D, x_E), \quad (4.14)$$

$$C_9^\gamma = \mathcal{N} \frac{\Gamma^L}{6m_\Phi^2} \tilde{G}_9(x_D), \quad C_7 = \mathcal{N} \frac{\Gamma^L}{6m_\Phi^2} F_7(x_D), \quad C_8 = -\mathcal{N} \frac{\Gamma^L}{2m_\Phi^2} F_7(x_D), \quad (4.15)$$

$$C_9'^{\text{box}} = C_9^{\text{box}} (L \leftrightarrow R), \quad C_{10}'^{\text{box}} = -C_{10}^{\text{box}} (L \leftrightarrow R), \quad (4.16)$$

$$C_9'^\gamma = C_9^\gamma (L \leftrightarrow R), \quad C_{7,8}' = C_{7,8} (L \leftrightarrow R). \quad (4.17)$$

- $b \rightarrow s\nu\bar{\nu}$ (see Eqs. (2.19)-(2.20))

$$C_L = -\mathcal{N} \frac{\Gamma^L |\Gamma_\mu^L|^2}{32\pi\alpha_{\text{EM}}m_\Phi^2} F(x_D, x_E), \quad C_R = -\mathcal{N} \frac{\Gamma^R |\Gamma_\mu^L|^2}{32\pi\alpha_{\text{EM}}m_\Phi^2} F(x_D, x_E). \quad (4.18)$$

- $B_s - \bar{B}_s$ (see Eqs. (2.23)-(2.28))

$$C_1 = \frac{|\Gamma^L|^2}{128\pi^2 m_\Phi^2} F(x_D), \quad C_5 = -\frac{\Gamma^L \Gamma^R}{32\pi^2 m_\Phi^2} F(x_D), \quad \tilde{C}_1 = \frac{|\Gamma^R|^2}{128\pi^2 m_\Phi^2} F(x_D), \quad (4.19)$$

⁹Note that the effect in scalar and magnetic operators can also be suppressed if $\Gamma_{b,s}^R = 0$ or very small. However, we decided to focus on option with $\lambda_{L,R}^D$ being very small.

where the (simplified) loop function are defined in Appendix B. In addition there are contributions to the C_1 analogue in $D^0 - \bar{D}^0$ mixing obtained by substituting $L_1^b \rightarrow L_1^c$ and $L_1^s \rightarrow L_1^u$ within Γ^L .

In the charged-lepton sector $SU(2)$ breaking effects (encoded in $\lambda_{L,R}^E$) can give a sizable chiral enhancement of the NP effect in a_μ (see Eq. (2.30)) such that the long-standing anomaly in this channel can be addressed. In general one can parametrize the rotation matrices as

$$W^{E_{L,R}} = \begin{pmatrix} \cos(\theta_{L,R}) & -\sin(\theta_{L,R}) \\ \sin(\theta_{L,R}) & \cos(\theta_{L,R}) \end{pmatrix}, \quad (4.20)$$

leading to

$$\begin{aligned} L_1^\mu &= \Gamma_\mu^L \cos \theta_L, & L_2^\mu &= -\Gamma_\mu^L \sin \theta_L, & L^\nu &= \Gamma_\mu^L, \\ R_1^\mu &= \Gamma_\mu^R \sin \theta_R, & R_2^\mu &= \Gamma_\mu^R \cos \theta_R. \end{aligned} \quad (4.21)$$

In our analysis we will consider a simplified setup with $\lambda_R^E = -\lambda_L^E \equiv \lambda^E$ that maximizes the effect in a_μ (which at leading order in v is proportional to $\lambda_R^E - \lambda_L^E$). In this approximation we have for

- a_μ (see Eq. (2.30))

$$\Delta a_\mu = \frac{m_\mu^2}{8\pi^2 m_\Phi^2} \left[(|\Gamma_\mu^L|^2 + |\Gamma_\mu^R|^2) F_7(x_E) + \frac{8}{\sqrt{2}} \frac{v \lambda^E}{m_\mu} \Gamma_\mu^L \Gamma_\mu^R G_7(x_E) \right], \quad (4.22)$$

where we have assumed real values for the couplings, implying a vanishing d_μ . Let us stress that the contributions proportional to $v \lambda^E$, coming from $SU(2)$ breaking terms, is chirally enhanced can give a sizable effect that can explain the a_μ anomaly.

- $Z \rightarrow \mu^+ \mu^-$ (see Eqs. (2.35)-(2.36))

$$\Delta g_{\mu_L}(m_Z^2) = -\frac{|\Gamma_\mu^L|^2}{32\pi^2} \left[\frac{m_Z^2}{m_\Phi^2} \left((1 - 2s_W^2) \tilde{G}_9(x_E) + \frac{2}{3} \left(\frac{v \lambda^E}{m_E} \right)^2 F_9(x_E) \right) + \left(\frac{v \lambda^E}{m_E} \right)^2 F_Z(x_E) \right], \quad (4.23)$$

$$\Delta g_{\mu_R}(m_Z^2) = \frac{|\Gamma_\mu^R|^2}{32\pi^2} \left[\frac{m_Z^2}{m_\Phi^2} \left(2s_W^2 \tilde{G}_9(x_E) + \frac{2}{3} \left(\frac{v \lambda^E}{m_E} \right)^2 F_9(x_E) \right) + \left(\frac{v \lambda^E}{m_E} \right)^2 F_Z(x_E) \right], \quad (4.24)$$

where the simplified loop function $F_Z(x_E)$ has been defined in Appendix B. The results for $Z \rightarrow b\bar{b}$ couplings can be easily obtained by suitable substitutions. Note that in our approximation of $\lambda_{L,R}^D = 0$ the correction to the $Z\bar{s}b$ vertex vanishes at $q^2 = 0$. Note that the UV divergences cancel as required, once for the couplings in Eq. (2.34) the relations

$$g^{\Psi, L(R)} = W^{E_{L(R)}} \dagger \begin{pmatrix} g_{\Psi_{L,2}} & 0 \\ 0 & g_{\Psi_e} \end{pmatrix} W^{E_{L(R)}} = W^{E_{L(R)}} \dagger \begin{pmatrix} g_{\mu_L}^{\text{SM}} & 0 \\ 0 & g_{\mu_R}^{\text{SM}} \end{pmatrix} W^{E_{L(R)}}, \quad (4.25)$$

and $g_\Phi = 0$ are used. Thus the finiteness of the result can be traced by to the unitarity of the matrices W .

4.3 Phenomenology

We are now ready to consider the phenomenology of our 4th generation model. For this purpose we will perform a combined fit to all the relevant and available experimental data, as briefly reviewed in Sec. 3. We perform this fit using the publicly available `HEPfit` package [172], performing a Markov Chain Monte Carlo (MCMC) analysis employing the Bayesian Analysis Toolkit (BAT) [173].

Let us first choose specific values for the masses of the scalar Φ and the fermions Ψ . As observed in Ref. [81] a large splitting between the scalar mass and the vector-like lepton mass with respect to the vector-like quark masses is welcome to suppress the relative effect in Δm_{B_s} . Since the vector-like quarks should not be too light anyway because of direct LHC searches [174, 175] we choose $m_\Phi \simeq m_E \simeq 450 \text{ GeV}$ ¹⁰ and $m_D = 3.15 \text{ TeV}$, corresponding to $x_{E,L} \simeq 1$ and $x_D \simeq 50$. These values are well beyond the reach of direct searches at LHC: Concerning $m_{E,L}$ the bounds come from Drell-Yan production of the new fermions which are subsequently decaying in the neutral scalar and SM leptons. Therefore, the collider signature is similar to the one of MSSM slepton [176, 177]¹¹.

Turning to the coupling of the new scalars and fermions to quarks and muons, we assume a flatly distributed priors within the range $|\Gamma| \leq 1.5$ such that perturbativity is respected. The marginalized posterior probability distribution for all NP couplings, together with the correlations among them, can be found in Appendix E. In the rest of this section we will focus on one particular benchmark point, that we selected because it lies within all the 1σ regions of the combined posterior distributions for the NP couplings (see Fig. 10). The benchmark values are

$$|\Gamma_\mu^L| = 1.5, \quad |\Gamma_\mu^R| = 1.4, \quad \lambda^E = 0.0015, \quad \Gamma^L = -1.0, \quad \Gamma^R = -0.12 \quad (4.26)$$

assuming real values for all couplings. Note that the small value for λ^E is obtained from the fit due to its correlation with $|\Gamma_\mu^R|$. As can be seen from the combined posterior distribution of these 2 parameters shown in Fig. 10, higher values of λ^E would require lower values of $|\Gamma_\mu^R|$, which is disfavored by the current fit to $b \rightarrow s\ell^+\ell^-$ data.

We observe that it is extremely important to allow for a right-handed coupling Γ_μ^R together a mixing coupling λ^E in the muon sector such that a_μ can be explained. This

¹⁰Nearly degenerate masses $m_\Phi \simeq m_E$ are also welcome in the light of the dark matter relic density since the stable Φ is a suitable DM candidate. In fact, for $m_\Phi = 450 \text{ GeV}$, $450 \leq m_E \leq 520 \text{ GeV}$ the model allows for an efficient annihilation such that one does not over-shoot the matter density of the universe for order one Γ couplings.

¹¹A detailed study recasting these MSSM analysis for our model has been performed in Refs. [101, 102], finding $m_E \gtrsim m_\Phi = 450 \text{ GeV}$ as an allowed solution.

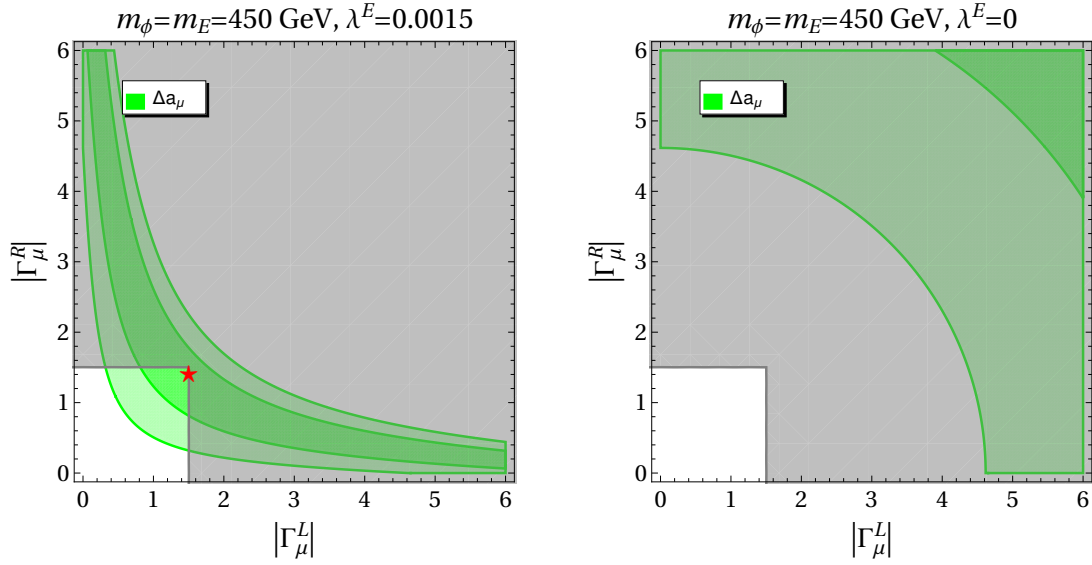


Figure 5. Left panel: allowed region for the coupling strength to the muon $|\Gamma_\mu^L|$ from the muon anomalous magnetic moment as a function of $|\Gamma_\mu^R|$, assuming $m_\phi = 450 \text{ GeV}$, $x^E=1$ and $\lambda^E = 0.0015$. The excluded region due to the requirement of perturbativity for $|\Gamma_\mu^{L,R}|$ is given in gray. Dark (light) green corresponds to 1σ (2σ) region. The red star marks the benchmark point $(1.5, 1.4)$. Right panel: same as the left panel, but assuming $\lambda^E = 0$.

can be seen from the fit in the $(|\Gamma_\mu^L|, |\Gamma_\mu^R|)$ -plane from the left panel of Fig. 5. In the case with $\lambda^E = 0.0015$, corresponding to the benchmark point reported in Eq. (4.26), one can see that it is possible to explain the deviation in a_μ by means of couplings of order unity. However, the situation changes significantly if one did not allow the presence of a coupling of the vector-like leptons to the SM Higgs. As shown in the right panel of Fig. 5, with $\lambda^E = 0$, it is not possible to obtain couplings that are perturbative and capable to give a satisfactory explanation of the anomalous magnetic moment of the muon at the same time. The presence of Γ_μ^R ameliorates the tension, but it is still not sufficient by itself to address the anomaly.

Also in the quark sector right-handed couplings are needed to address the B anomalies without spoiling at the same time the measurement for ΔM_s . This is particularly evident by looking at the left panel of Fig. 6, where the region allowed by both $b \rightarrow s\mu^+\mu^-$ transitions and $B_s - \bar{B}_s$ is shown. Indeed, if one performs a separate fit to $b \rightarrow s\mu^+\mu^-$ transitions and ΔM_s as shown in the right panel of Fig. 6, it is evident that the two channels are incompatible as long as one assumes a vanishing coupling to right-handed bottom and strange quarks, i.e. $\Gamma^R = 0$.

The preference for non-zero couplings (i.e. beyond the SM effects) is in general driven by Δa_μ , the angular analyses of $B \rightarrow K^*\mu^+\mu^-$ and $B_s \rightarrow \phi\mu^+\mu^-$, the branching fraction of

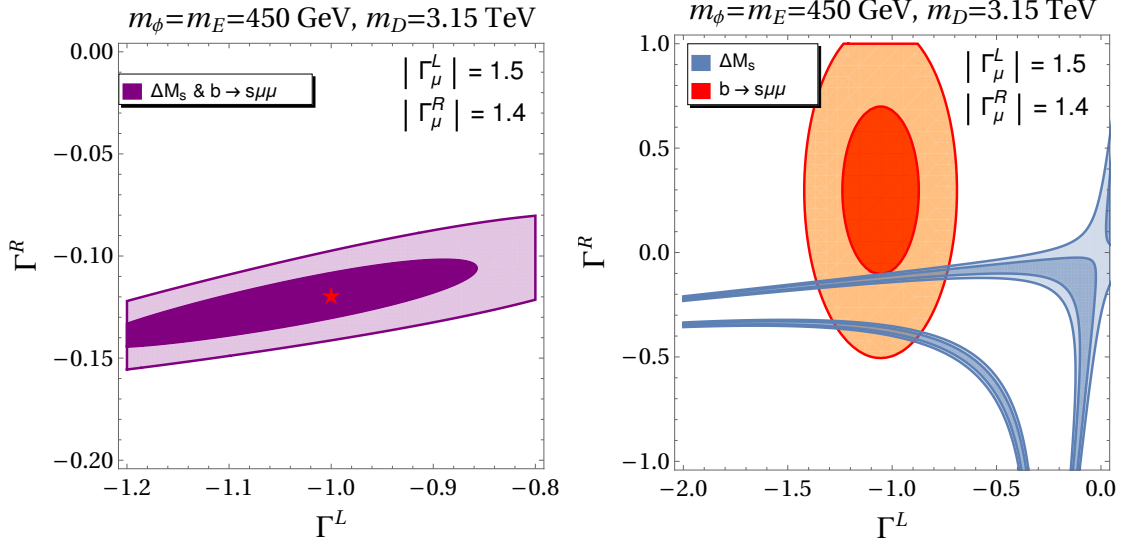


Figure 6. Left panel: Allowed region for the coupling $\Gamma^L \equiv \Gamma_b^L \Gamma_s^{L*}$ and $\Gamma^R \equiv \Gamma_b^R \Gamma_s^{R*}$ from $B_s - \bar{B}_s$ mixing and $b \rightarrow s\mu^+\mu^-$ data for $m_\phi = m_E = 450$ GeV, $m_D = 3.15$ TeV, $|\Gamma_\mu^L| = 1.5$ and $|\Gamma_\mu^R| = 1.4$. The red star marks the values at our benchmark point $(-1, -0.12)$. The dark (light) purple regions is preferred at the 1σ (2σ) level. Right panel: same as the left panel, but showing separately the allowed regions coming from $B_s - \bar{B}_s$ mixing (in blue) and $b \rightarrow s\mu^+\mu^-$ data (in red). The upper branch allowed by $B_s - \bar{B}_s$ mixing corresponds to the one shown on the left.

$B_s \rightarrow \mu^+\mu^-$ and the ratios R_K and R_{K^*} . On the other hand, the experimental constraints coming from $b \rightarrow s\gamma$ and $B \rightarrow K^{(*)}\nu\bar{\nu}$ and ΔM_{B_s} set bounds on $\Gamma^{L,R}$ and $|\Gamma_\mu^L|$ that are less stringent than the ones obtained by the inclusion of the aforementioned channels involving $b \rightarrow s$ transitions in our setup with $\lambda_{L,R}^D = 0$. Analogously, the constraints from $Z \rightarrow \mu^+\mu^-$ are found to give negligible constraints on $|\Gamma_\mu^{L,R}|$. Concerning $D_0 - \bar{D}_0$ mixing, we recall that Eq. (4.11) implies a relation between $\Gamma^L \equiv L_1^b L_1^{s*}$ and $L_1^{u,c}$. Exploiting the fact that only the product of $L_1^b L_1^{s*}$ enters $b \rightarrow s\ell^+\ell^-$, together with the suppression of the L_1^b in $L_1^{u,c}$ by small CKM factors ($\mathcal{O}(\lambda^3)$ and $\mathcal{O}(\lambda^2)$, respectively), it is possible arrange the contributions to Γ^L in such a way that the constraint imposed by $D_0 - \bar{D}_0$ mixing is automatically satisfied.

We conclude this section by giving the results for some important observables (within our model) obtained from the global fit, namely

$$\begin{aligned}
 R_K[1.1, 6] &= 0.781(45), & R_{K^*}[1.1, 6] &= 0.885(39), & \bar{\mathcal{B}}(B_s \rightarrow \mu^+\mu^-) &= 3.30(21) \cdot 10^{-9}, \\
 P'_5[4, 6] &= -0.454(69), & P'_5[6, 8] &= -0.626(59), \\
 \Delta a_\mu &= 235(87) \cdot 10^{-11}, & R_{\Delta M_s} &= -0.02(8).
 \end{aligned} \tag{4.27}$$

All the predictions for these observables are compatible at the 1σ level with their experimental measurements described in Sec. 3, except for R_{K^*} which is compatible only at the $\sim 2\sigma$ level. However, this is expected both from the global fit and from our specific model: As can be seen from the right panel of Fig. 6, there is no overlap of the 1σ regions from $b \rightarrow s\mu^+\mu^-$ data and ΔM_s in our model. Furthermore, since our model only allows for NP in muons (neglecting Z, γ penguin effects), some small tensions are generated since flavour conserving $b \rightarrow s\mu^+\mu^-$ data prefers a smaller value of R_K than the one recently measured.

5 Conclusions and Outlook

In this article we have studied in details the possibility that the intriguing anomalies in $b \rightarrow s\ell^+\ell^-$ processes are explained via box diagrams involving new scalars and fermions. Within this setup we have generalized previous analysis [78, 79, 81] to include couplings of the new particles to right-handed SM fermion and calculated the completely general expressions for the Wilson coefficients governing $b \rightarrow s$ processes ($b \rightarrow s\ell^+\ell^-$, $b \rightarrow s\nu\bar{\nu}$, $b \rightarrow s\gamma$ and $B_s - \bar{B}_s$ mixing). In addition, we have computed the effects in a_μ and $Z \rightarrow \mu^+\mu^-$ which unavoidably arise in such scenarios.

Furthermore, we have proposed a UV complete model containing a 4th vector-like generation of fermions and a new scalar, which is capable of explaining $b \rightarrow s\ell^+\ell^-$ data and a_μ . We applied the formula derived in our generic setup (see Sec. 2) to this model, illustrating their usefulness. In the following phenomenological analysis of our 4th generation model (see Sec. 4.3) we came to the conclusion that the $b \rightarrow s\ell^+\ell^-$ anomalies and a_μ can be explained simultaneously. As a benchmark point which can achieve this, and is consistent with direct LHC searches, we have used 450 GeV for the vector-like fermions and for the new scalar and $m_D = 3.15$ TeV for the vector like quarks (with order one couplings). We have observed that right-handed couplings in the muon sector allow to address the long-standing anomaly in a_μ without having to require too large lepton couplings, if one allows for interactions of the vector-like fermions with the SM Higgs. Interestingly, due to the new results from LHCb and BELLE [9, 10] the global fit to $b \rightarrow s\ell^+\ell^-$ data now prefers non-zero right-handed couplings to quarks and leptons as well, justifying the importance of our generalization of previous analysis performed in this work.

Our 4th generation model is also interesting since Φ is a viable (stable) Dark Matter candidate. We briefly showed that if the mass of Φ is close to the one of the vector-like leptons, the correct relic density can be obtained while respecting the limits from Dark Matter direct detection. However, a more detailed investigation in the future seems worthwhile.

We conclude observing that our formalism can be directly applied to $b \rightarrow d\ell^+\ell^-$ transitions. In fact, it leads to correlated effects in Kaon physics [178] if one aims at

explaining the slight tensions in $B \rightarrow \pi \mu^+ \mu^-$ [179] simultaneously with the ones in $b \rightarrow s \ell^+ \ell^-$ data. Furthermore, our setup and results can also be used for addressing the tension between theory and experiment in ϵ'/ϵ [180, 181]¹². Here, as a special case of our generic approach, the MSSM has already been studied with the conclusion that it can provide a valid explanation of the anomaly [184–186].

Note added: After publication of this article, the g-2 collaboration at Fermilab released a new measurement of a_μ [187], which together with the theory consensus of Ref. [188] leads to a tension of 4.2σ . Furthermore, the LHCb collaboration updated the measurements of $R(K)$ [189] and released the first measurement of P'_5 in $B^+ \rightarrow K^{+*} \mu \mu$ [190]. Note that this does not change the conclusions of our article and the impact on the numeric is very small. However, this gives additional support to our 4th generation model which can account for $(g-2)_\mu$ and B -anomalies.

Acknowledgments

We thank Lorenzo Calibbi and Mauro Valli for useful discussions during the completion of the manuscript. The work of A.C. is supported by an Ambizione Grant (PZ00P2_154834) and a Professorship Grant (PP00P2_176884) of the Swiss National Science Foundation. P.A., M.F. and F.M. acknowledge the financial support from MINECO grant FPA2016-76005-C2-1-P, Maria de Maetzu program grant MDM-2014-0367 of ICCUB and 2017 SGR 929.

A Fierz Identities

Here we list the Fierz identities for spinors used in the computations. With i, j, k and l representing Dirac indices here we find

$$(\gamma_\mu P_{L,R})_{ij} (\gamma_\mu P_{L,R})_{kl} = -(\gamma_\mu P_{L,R})_{il} (\gamma_\mu P_{L,R})_{kj} \quad (\text{A.1})$$

$$(\gamma_\mu P_{L,R})_{ij} (\gamma_\mu P_{R,L})_{kl} = 2(P_{R,L})_{il} (P_{L,R})_{kj} \quad (\text{A.2})$$

$$(P_{L,R})_{ij} (P_{L,R})_{kl} = \frac{1}{2} (P_{L,R})_{il} (P_{L,R})_{kj} + \frac{1}{8} (\sigma_{\mu\nu})_{il} (\sigma_{\mu\nu} P_{L,R})_{kj} \quad (\text{A.3})$$

$$(P_{L,R})_{ij} (P_{R,L})_{kl} = \frac{1}{2} (\gamma_\mu P_{R,L})_{il} (\gamma_\mu P_{L,R})_{kj} \quad (\text{A.4})$$

$$(\sigma_{\mu\nu})_{ij} (\sigma_{\mu\nu} P_{L,R})_{kl} = 6(\gamma_\mu P_{L,R})_{il} (\gamma_\mu P_{L,R})_{kj} - \frac{1}{2} (\sigma_{\mu\nu})_{il} (\sigma_{\mu\nu} P_{L,R})_{kj} , \quad (\text{A.5})$$

¹²Note that calculations using chiral perturbation theory [182, 183] instead are consistent with both the experimental measurement and the SM results of Refs. [180, 181].

where $P_{L,R} = (1 \mp \gamma_5)/2$ and $\sigma_{\mu\nu} = \frac{i}{2} [\gamma_\mu, \gamma_\nu]$. When dealing with diagrams with crossed fermion lines, one needs Fierz identities involving charge conjugation matrices. Here, exchanging the second and the third Dirac index we find

$$(\gamma_\mu P_{L,R} C)_{ij} (C \gamma_\mu P_{L,R})_{kl} = -2 (P_{R,L})_{ik} (P_{L,R})_{jl} \quad (\text{A.6})$$

$$(\gamma_\mu P_{L,R} C)_{ij} (C \gamma_\mu P_{R,L})_{kl} = -(\gamma_\mu P_{L,R})_{ik} (\gamma_\mu P_{R,L})_{jl} \quad (\text{A.7})$$

$$(P_{L,R} C)_{ij} (C P_{L,R})_{kl} = \frac{1}{2} (P_{L,R})_{ik} (P_{L,R})_{jl} - \frac{1}{8} (\sigma_{\mu\nu})_{ik} (\sigma_{\mu\nu} P_{L,R})_{jl} \quad (\text{A.8})$$

$$(P_{L,R} C)_{ij} (C P_{R,L})_{kl} = -\frac{1}{2} (\gamma_\mu P_{R,L})_{ik} (\gamma_\mu P_{R,L})_{jl} , \quad (\text{A.9})$$

with the charge conjugation matrix defined as $C = i\gamma_0\gamma_2$.

B Loop Functions

Here we list the dimensionless loop functions introduced in Sections 2 and 4. The loop functions appearing in box diagrams that involve four different masses are defined as

$$\begin{aligned} F(x, y, z) &= \frac{x^2 \log(x)}{(x-1)(x-y)(x-z)} + \frac{y^2 \log(y)}{(y-1)(y-x)(y-z)} + \frac{z^2 \log(z)}{(z-1)(z-x)(z-y)} , \\ G(x, y, z) &= 2 \left(\frac{x \log(x)}{(x-1)(x-y)(x-z)} + \frac{y \log(y)}{(y-1)(y-x)(y-z)} + \frac{z \log(z)}{(z-1)(z-x)(z-y)} \right) , \end{aligned} \quad (\text{B.1})$$

which in the equal mass limit read

$$F(1, 1, 1) = -G(1, 1, 1) = \frac{1}{3} . \quad (\text{B.2})$$

In the presence of only three different masses in the loop, one gets the functions

$$\begin{aligned} F(x, y) \equiv F(x, y, 1) &= \frac{1}{(1-x)(1-y)} + \frac{x^2 \log(x)}{(1-x)^2(x-y)} + \frac{y^2 \log(y)}{(1-y)^2(y-x)} , \\ G(x, y) \equiv G(x, y, 1) &= 2 \left(\frac{1}{(1-x)(1-y)} + \frac{x \log(x)}{(1-x)^2(x-y)} + \frac{y \log(y)}{(1-y)^2(y-x)} \right) , \end{aligned} \quad (\text{B.3})$$

while, in the presence of only two different masses in the loop, one gets

$$\begin{aligned} F(x) \equiv F(x, x) &= \frac{x+1}{(x-1)^2} - \frac{2x \log(x)}{(x-1)^3} , \\ G(x) \equiv G(x, x) &= \frac{2}{(x-1)^2} - \frac{(x+1) \log(x)}{(x-1)^3} . \end{aligned} \quad (\text{B.4})$$

The loop functions appearing in photon- and gluon-penguin diagrams are defined as

$$\begin{aligned}
F_7(x) &= \frac{x^3 - 6x^2 + 3x + 2 + 6x \log x}{12(x-1)^4}, & \tilde{F}_7(x) &= x^{-1}F_7(x^{-1}), \\
G_7(x) &= \frac{x^2 - 4x + 3 + 2 \log x}{8(x-1)^3}, & \tilde{G}_7(x) &= \frac{x^2 - 2x \log x - 1}{8(x-1)^3}, \\
F_9(x) &= \frac{-2x^3 + 9x^2 - 18x + 11 + 6 \log x}{36(x-1)^4}, & \tilde{F}_9(x) &= x^{-1}F_9(x^{-1}), \\
G_9(x) &= \frac{-16x^3 + 45x^2 - 36x + 7 + 6(2x-3)x^2 \log x}{36(x-1)^4}, & \tilde{G}_9(x) &= x^{-1}G_9(x^{-1}),
\end{aligned} \tag{B.5}$$

which in the equal mass limit read

$$F_7(1) = \tilde{F}_7(1) = \frac{G_7(1)}{2} = \tilde{G}_7(1) = -F_9(1) = -\tilde{F}_9(1) = \frac{G_9(1)}{3} = \frac{\tilde{G}_9(1)}{3} = \frac{1}{24}. \tag{B.6}$$

Finally, the loop functions for the calculation of Z -penguins are defined as

$$\begin{aligned}
G_Z(x, y) &= xF_V(x, y) + x \leftrightarrow y, \\
F_Z(x, y, m) &\equiv \bar{F}_Z(x, y) - \overline{div}_\varepsilon = (x^2F_V(x, y) + x \leftrightarrow y) - \overline{div}_\varepsilon, \\
H_Z(x, y, m) &\equiv \bar{H}_Z(x, y) + \overline{div}_\varepsilon = (yF_V(x, y) + x \leftrightarrow y) + 1 + \overline{div}_\varepsilon, \\
I_Z(x, m) &\equiv \bar{I}_Z(x) + \overline{div}_\varepsilon = \frac{x}{x-1} - x^2F_V(x, 1) + \overline{div}_\varepsilon, \\
\tilde{G}_Z(x, y) &= xK_V(x, y) + x \leftrightarrow y, \\
\tilde{F}_Z(x, y) &= \left(x^2K_V(x, y) - \frac{x^2}{x-y}F_V(x, y) \right) + x \leftrightarrow y, \\
\tilde{H}_Z(x, y) &= \left(\frac{x^2y}{(y-1)(x-y)^2} - \frac{x^2y^2(3x-y-2)\log(x)}{(x-1)^2(x-y)^3} \right) + x \leftrightarrow y,
\end{aligned} \tag{B.7}$$

where we have defined $\overline{div}_\varepsilon = \Delta_\varepsilon - \log\left(\frac{m^2}{\mu^2}\right)$ and

$$F_V(x, y) = \frac{\log(x)}{(x-1)(x-y)}, \quad K_V(x, y) = \frac{(x^2 + xy - 2y)\log(x)}{(x-1)^2(x-y)^3} - \frac{1}{(x-1)(x-y)^2}. \tag{B.8}$$

It is interesting to notice that the following relations hold between particular limits of the penguin induced functions:

$$\begin{aligned}
H_Z\left(\frac{m^2}{n^2}, \frac{m^2}{n^2}, m\right) &= I_Z\left(\frac{m^2}{n^2}, n\right), \\
-\frac{m^2}{n^2}G_Z\left(\frac{m^2}{n^2}, \frac{m^2}{n^2}\right) &+ \frac{1}{2}F_Z\left(\frac{m^2}{n^2}, \frac{m^2}{n^2}, n\right) + \frac{1}{4}H_Z\left(\frac{m^2}{n^2}, \frac{m^2}{n^2}, m\right) + \frac{1}{4}I_Z\left(\frac{m^2}{n^2}, n\right) = 0, \\
\frac{1}{2}x\tilde{G}_Z(x, x) - \frac{1}{3}\tilde{F}_Z(x, x) &= \tilde{G}_9(x),
\end{aligned}$$

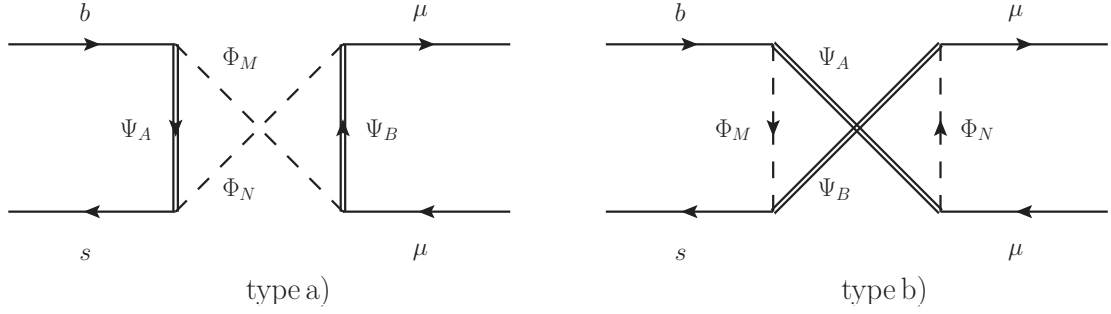


Figure 7. Crossed box diagrams contributing to $b \rightarrow s\mu^+\mu^-$ transitions. The diagram on the left appears in models with real scalars, while the one on the right can be constructed in models with Majorana fermions.

$SU(3)$, type a)	Ψ_A	Ψ_B	Φ_M	Φ_N	$SU(3)$, type b)	Ψ_A	Ψ_B	Φ_M	Φ_N	χ
I	3	1	1	1	I	1	1	3	1	1
III	3	8	8	8	III	8	8	3	8	4/3

Table 5. Table of $SU(3)$ -factors entering the box induced Wilson coefficients involved in $b \rightarrow s$ transitions for real scalars, type a), and Majorana fermions, type b). The numbers of each representation refer to the ones in Table 1.

$$\frac{1}{6} \tilde{F}_Z(x, x) = F_9(x). \quad (\text{B.9})$$

$$\frac{1}{6x} \tilde{H}_Z(x, x) = \tilde{F}_9(x). \quad (\text{B.10})$$

Moreover, it is useful to define the limit

$$F_Z(x) \equiv \overline{F}_Z(x, x) = \frac{x}{x-1} + \frac{(x-2)x \log x}{(x-1)^2}. \quad (\text{B.11})$$

Finally, the equal mass limits read

$$G_Z(1, 1) = \frac{\overline{F}_Z(1, 1)}{3} = -\overline{H}_Z(1, 1) = -\overline{I}_Z(1) = 6\tilde{G}_Z(1, 1) = -2\tilde{F}_Z(1, 1) = -2\tilde{H}_Z(1, 1) = \frac{1}{2}. \quad (\text{B.12})$$

C Real Scalars and Majorana Fermions

If the NP fields have the appropriate quantum numbers they can be either real scalars or Majorana fermions. If this is the case, crossed diagrams as shown in Fig. 7 can be constructed and contribute to $b \rightarrow s\mu^+\mu^-$ transitions in addition to the ones shown in Fig. 1. Similarly, there are contributions from crossed boxes to $B_s - \bar{B}_s$ mixing (in addition to the ones in Fig. 3) arising due to the diagrams in Fig. 8.

C.1 $b \rightarrow s\mu^+\mu^-$

In $b \rightarrow s\mu^+\mu^-$ the possible representations that give rise to additional crossed diagrams with real scalars or Majorana fermions are listed in Tab. 5. For type a) the only possibility is to have real scalars, while for type b) one can only have crossed diagrams in the presence of Majorana fermions.

The contribution to the Wilson coefficients stemming from the diagrams in Fig. 7a) corresponds to the ones listed for a)-type in Eqs. (2.4)-(2.7), after inverting $M \leftrightarrow N$ in the muon couplings and changing $F(x_{AM}, x_{BM}, x_{NM}) \rightarrow -F(x_{AM}, x_{BM}, x_{NM})$. For case b) (see right diagram in Fig. 7) the Wilson coefficients are given by

$$C_9^{\text{box } b)} = -\mathcal{N} \frac{\chi L_{BM}^{s*} L_{AM}^b}{32\pi\alpha_{\text{EM}} m_{\Phi_M}^2} \left[L_{BN}^{\mu*} L_{AN}^\mu \frac{m_{\Psi_A} m_{\Psi_B}}{m_{\Phi_M}^2} G(x_{AM}, x_{BM}, x_{NM}) - R_{BN}^{\mu*} R_{AN}^\mu F(x_{AM}, x_{BM}, x_{NM}) \right], \quad (\text{C.1})$$

$$C_{10}^{\text{box } b)} = \mathcal{N} \frac{\chi L_{BM}^{s*} L_{AM}^b}{32\pi\alpha_{\text{EM}} m_{\Phi_M}^2} \left[L_{BN}^{\mu*} L_{AN}^\mu \frac{m_{\Psi_A} m_{\Psi_B}}{m_{\Phi_M}^2} G(x_{AM}, x_{BM}, x_{NM}) + R_{BN}^{\mu*} R_{AN}^\mu F(x_{AM}, x_{BM}, x_{NM}) \right], \quad (\text{C.2})$$

$$C_S^{\text{box } b)} = \mathcal{N} \frac{\chi L_{BM}^{s*} L_{AM}^b}{16\pi\alpha_{\text{EM}} m_{\Phi_M}^2} \left[R_{BN}^{\mu*} L_{AN}^\mu F(x_{AM}, x_{BM}, x_{NM}) + L_{BN}^{\mu*} R_{AN}^\mu \frac{m_{\Psi_A} m_{\Psi_B}}{2m_{\Phi_M}^2} G(x_{AM}, x_{BM}, x_{NM}) \right], \quad (\text{C.3})$$

$$C_P^{\text{box } b)} = \mathcal{N} \frac{\chi L_{BM}^{s*} L_{AM}^b}{16\pi\alpha_{\text{EM}} m_{\Phi_M}^2} \left[R_{BN}^{\mu*} L_{AN}^\mu F(x_{AM}, x_{BM}, x_{NM}) - L_{BN}^{\mu*} R_{AN}^\mu \frac{m_{\Psi_A} m_{\Psi_B}}{2m_{\Phi_M}^2} G(x_{AM}, x_{BM}, x_{NM}) \right], \quad (\text{C.4})$$

$$C_T^{\text{box } b)} = -\mathcal{N} \frac{\chi L_{BM}^{s*} R_{AM}^b L_{BN}^{\mu*} R_{AN}^\mu}{16\pi\alpha_{\text{EM}} m_{\Phi_M}^2} \frac{m_{\Psi_A} m_{\Psi_B}}{m_{\Phi_M}^2} G(x_{AM}, x_{BM}, x_{NM}), \quad (\text{C.5})$$

$$C_{9,S}^{\prime\text{box}} = C_{9,S}^{\text{box}} (L \leftrightarrow R), \quad C_{P,10}^{\prime\text{box}} = -C_{P,10}^{\text{box}} (L \leftrightarrow R), \quad (\text{C.6})$$

C.2 $B_s - \bar{B}_s$ mixing

For B_s mixing we can either have real scalars or Majorana fermions. In Tab. 6 we list the possible representations of the diagrams in Fig. 8 writing explicitly if we have a real scalar contribution (diagrams on the left side of the figure) or a Majorana fermion (diagrams on the right). The WCs for real scalar crossed diagrams correspond to the ones listed in Eqs. (2.4)-(2.7), after inverting $M \leftrightarrow N$ in two of the four couplings and changing $F(x_{AM}, x_{BM}, x_{NM}) \rightarrow -F(x_{AM}, x_{BM}, x_{NM})$, whereas matching to the generic Lagrangian

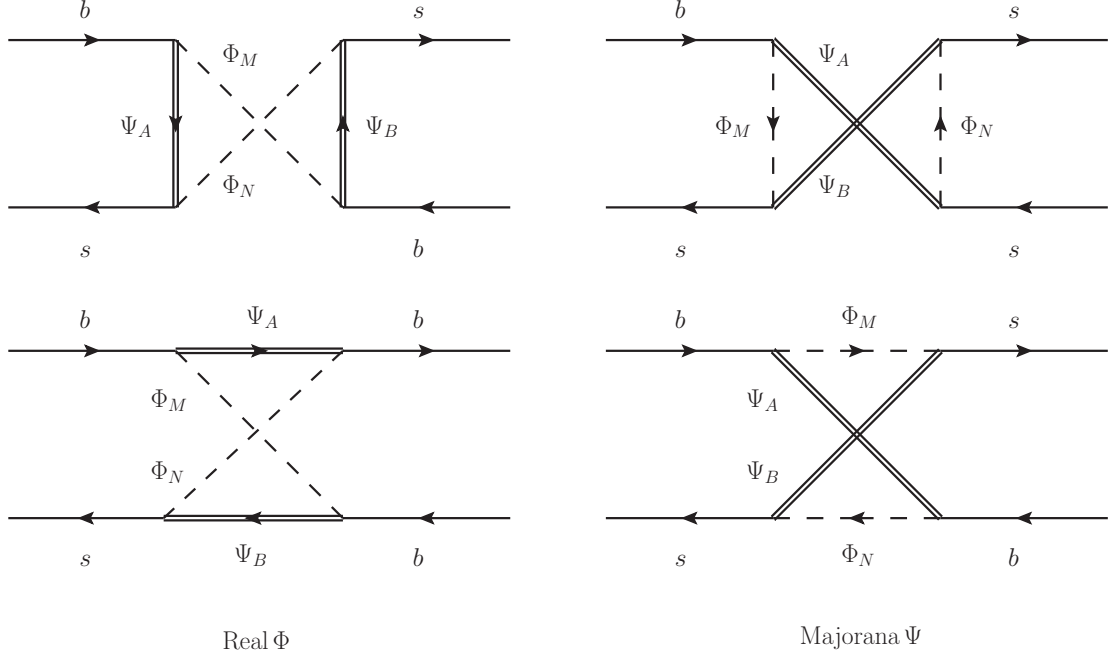


Figure 8. Box diagrams contributing to $B_s - \bar{B}_s$ mixing. The diagram on the left is relative to models with real scalars, while the one on the right refers to models with Majorana fermions.

$SU(3)$	Ψ_A	Ψ_B	Φ_M	Φ_N	χ_{BB}^M	$\tilde{\chi}_{BB}^M$	
I	3	3	1	1	1	0	Real Φ
II	1	1	3	3	0	1	Majorana Ψ
III	3	3	8	8	5/18	-1/6	Real Φ
IV	8	8	3	3	-1/6	5/18	Majorana Ψ
V	3	3	(1,8)	(8,1)	1/6	-1/2	Real Φ
VI	(1,8)	(8,1)	3	3	-1/2	1/6	Majorana Ψ

Table 6. Table of $SU(3)$ -factors entering the box induced Wilson coefficients involved in $B_s - \bar{B}_s$ mixing for real scalars and Majorana fermions.

from Eq. (2.1) with the crossed fermion contributions, one obtains the following results for the coefficients:

$$C_1 = (\chi_{BB}^M + \tilde{\chi}_{BB}^M) \frac{L_{AN}^{s*} L_{BM}^b L_{AM}^{s*} L_{BN}^b}{128\pi^2 m_{\Phi_M}^2} \frac{m_{\Psi_A} m_{\Psi_B}}{m_{\Phi_M}^2} G(x_{AM}, x_{BM}, x_{NM}) , \quad (C.7)$$

$$C_{2,3} = -(\chi_{BB}^M + \tilde{\chi}_{BB}^M) \frac{R_{AN}^{s*} L_{BM}^b R_{AM}^{s*} L_{BN}^b}{64\pi^2 m_{\Phi_M}^2} \frac{m_{\Psi_A} m_{\Psi_B}}{m_{\Phi_M}^2} G(x_{AM}, x_{BM}, x_{NM}) , \quad (C.8)$$

$$C_4 = \frac{L_{AM}^b R_{AN}^b}{32\pi^2 m_{\Phi_M}^2} [\chi_{BB}^M L_{BM}^{s*} R_{BN}^{s*} - \tilde{\chi}_{BB}^M R_{BM}^{s*} L_{BN}^{s*}] F(x_{AM}, x_{BM}, x_{NM}) , \quad (C.9)$$

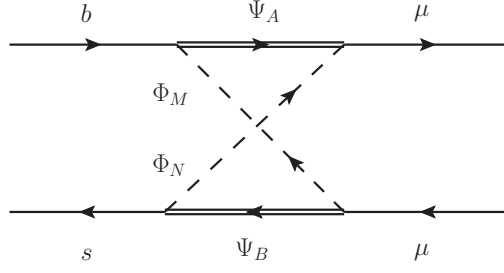


Figure 9. Crossed box diagrams contributing to $b \rightarrow s\mu^+\mu^-$ transitions. The diagram appears when a complex scalar couples to b, s quarks and its conjugate couples to the muons.

$$C_5 = \frac{L_{AM}^b R_{AN}^b}{32\pi^2 m_{\Phi_M}^2} [\tilde{\chi}_{BB}^M L_{BM}^{s*} R_{BN}^{s*} - \chi_{BB}^M R_{BM}^{s*} L_{BN}^{s*}] F(x_{AM}, x_{BM}, x_{NM}) , \quad (\text{C.10})$$

$$\tilde{C}_i = C_i(L \rightarrow R) , \quad \text{for } i = \{1, 2, 3\} , \quad (\text{C.11})$$

The corresponding contributions to $D_0 - \bar{D}_0$ mixing are obtained from Eqs. (2.22)-(2.28) via the replacements $s \rightarrow u$ and $b \rightarrow c$.

D Crossed Diagrams with Complex Scalars

There is also the possibility that a complex scalar couples to the down-type quarks whereas its hermitian conjugated version couples to muons. This means that the Lagrangian in Eq. (2.1) takes a slightly different form, namely

$$\begin{aligned} \mathcal{L}_{\text{int}} = & \left[\bar{\Psi}_A \left(L_{AM}^b P_L b + L_{AM}^s P_L s + R_{AM}^b P_R b + R_{AM}^s P_R s \right) \Phi_M \right. \\ & \left. + \bar{\Psi}_A \left(L_{AM}^\mu P_L + R_{AM}^\mu P_R \mu \right) \Phi_M^\dagger \right] + \text{h.c.} . \end{aligned} \quad (\text{D.1})$$

Also this Lagrangian generates a contribution to $b \rightarrow s\mu^+\mu^-$ via the diagram shown in Fig. 9. The possible representations under the $SU(3)$ of the new scalars and fermions in the loop are listed in Tab. 7. The corresponding Wilson Coefficients can be obtained from the ones calculated for the type b) diagrams in Eqs. (2.4)-(2.7) by exchanging $M \leftrightarrow N$ in the couplings R, L and replacing $F(x_{AM}, x_{BM}, x_{NM}) \rightarrow -F(x_{AM}, x_{BM}, x_{NM})$.

E Posterior Distributions

Here we show the 1D marginalized posterior distributions of the parameters from the global fit described in Sec. 4.1, together with the 2D combined correlations between these parameters. The results are summarized in Fig. 10. We recall that, for all couplings Γ , we imposed $|\Gamma| \leq 1.5$ such that perturbativity is satisfied. The consequences of such this choice are evident in the posterior distributions of Γ_μ^L , $|\Gamma_\mu^L|$ and $|\Gamma_\mu^R|$, which are truncated because of this reason.

$SU(3)$	Ψ_A	Ψ_B	Φ_M	Φ_N	χ
I	(1,3)	(3,1)	($\bar{3}$,1)	(1, $\bar{3}$)	1
II	(8,3)	(3,8)	($\bar{3}$,8)	(8, $\bar{3}$)	4/3
III	$\bar{3}$	$\bar{3}$	3	3	2

Table 7. Table of $SU(3)$ -factors entering the box induced Wilson coefficients involved in $b \rightarrow s$ transitions for crossed diagrams with complex scalars.

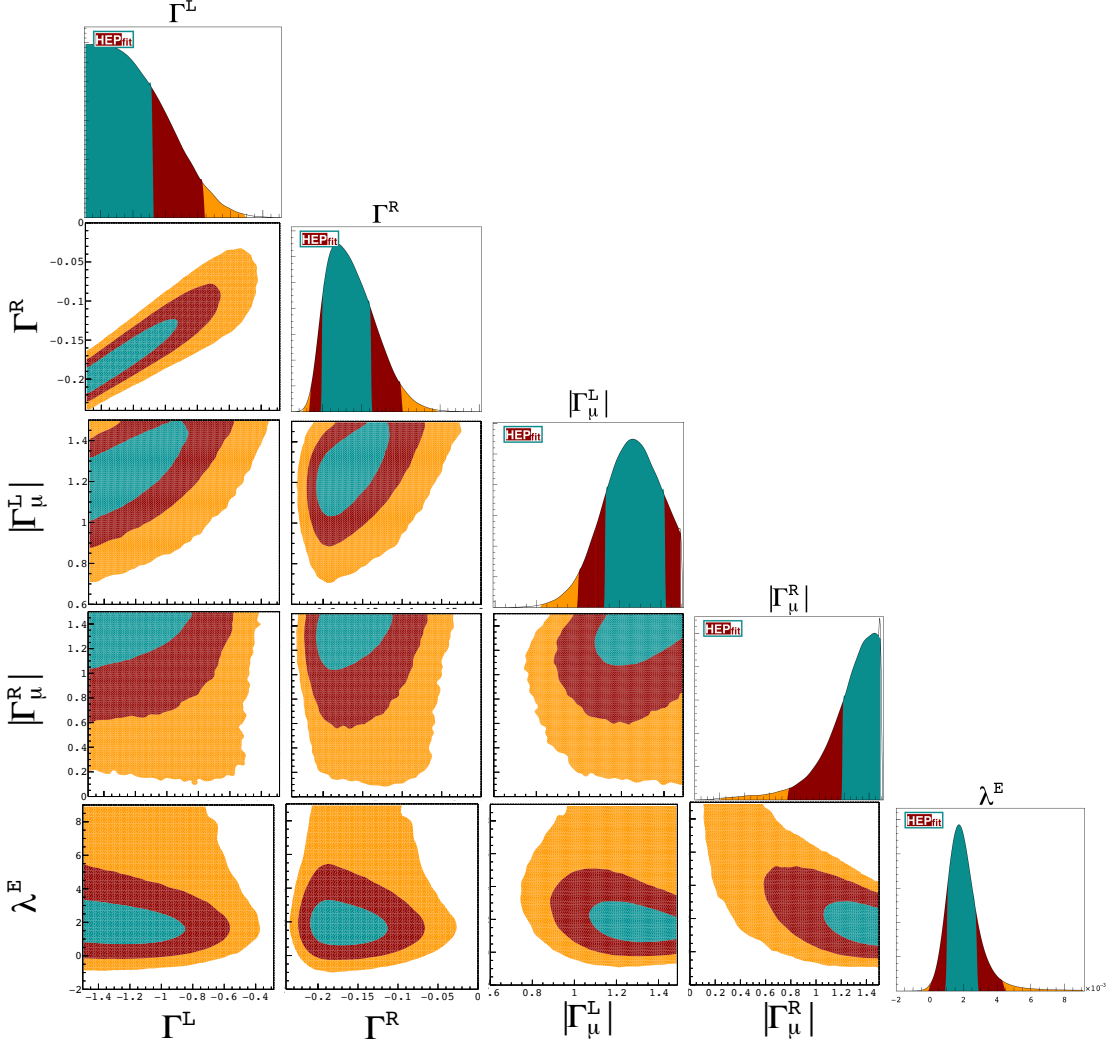


Figure 10. The 1D marginalized posterior distributions of the parameters from the fit described in sec. 4.1, together with the 2D correlations between them. The green, red and orange regions correspond to 68%, 95% and 99% probability regions, respectively.

References

- [1] B. Capdevila, A. Crivellin, S. Descotes-Genon, J. Matias and J. Virto, *Patterns of New Physics in $b \rightarrow s \ell^+ \ell^-$ transitions in the light of recent data*, *JHEP* **01** (2018) 093

- [1704.05340].
- [2] W. Altmannshofer, P. Stangl and D. M. Straub, *Interpreting Hints for Lepton Flavor Universality Violation*, *Phys. Rev.* **D96** (2017) 055008 [1704.05435].
 - [3] G. D’Amico, M. Nardecchia, P. Panci, F. Sannino, A. Strumia, R. Torre et al., *Flavour anomalies after the R_{K^*} measurement*, *JHEP* **09** (2017) 010 [1704.05438].
 - [4] G. Hiller and I. Nisandzic, *R_K and R_{K^*} beyond the standard model*, *Phys. Rev.* **D96** (2017) 035003 [1704.05444].
 - [5] L.-S. Geng, B. Grinstein, S. Jäger, J. Martin Camalich, X.-L. Ren and R.-X. Shi, *Towards the discovery of new physics with lepton-universality ratios of $b \rightarrow s\ell\ell$ decays*, *Phys. Rev.* **D96** (2017) 093006 [1704.05446].
 - [6] M. Ciuchini, A. M. Coutinho, M. Fedele, E. Franco, A. Paul, L. Silvestrini et al., *On Flavourful Easter eggs for New Physics hunger and Lepton Flavour Universality violation*, *Eur. Phys. J.* **C77** (2017) 688 [1704.05447].
 - [7] A. K. Alok, B. Bhattacharya, A. Datta, D. Kumar, J. Kumar and D. London, *New Physics in $b \rightarrow s\mu^+\mu^-$ after the Measurement of R_{K^*}* , *Phys. Rev.* **D96** (2017) 095009 [1704.07397].
 - [8] T. Hurth, F. Mahmoudi, D. Martinez Santos and S. Neshatpour, *Lepton nonuniversality in exclusive $b \rightarrow s\ell\ell$ decays*, *Phys. Rev.* **D96** (2017) 095034 [1705.06274].
 - [9] LHCb collaboration, *Search for lepton-universality violation in $B^+ \rightarrow K^+\ell^+\ell^-$ decays*, [1903.09252](#).
 - [10] BELLE collaboration, *Test of lepton flavor universality in $B \rightarrow K^*\ell^+\ell^-$ decays at Belle*, [1904.02440](#).
 - [11] HEAVY FLAVOR AVERAGING GROUP collaboration, *Averages of b -hadron, c -hadron, and τ -lepton properties as of summer 2016*, *Eur. Phys. J.* **C77** (2017) 895 [1612.07233].
 - [12] M. Algueró, B. Capdevila, A. Crivellin, S. Descotes-Genon, P. Masjuan, J. Matias et al., *Addendum: "Patterns of New Physics in $b \rightarrow s\ell^+\ell^-$ transitions in the light of recent data" and "Are we overlooking Lepton Flavour Universal New Physics in $b \rightarrow s\ell\ell$?"*, [1903.09578](#).
 - [13] A. K. Alok, A. Dighe, S. Gangal and D. Kumar, *Continuing search for new physics in $b \rightarrow s\mu\mu$ decays: two operators at a time*, [1903.09617](#).
 - [14] M. Ciuchini, A. M. Coutinho, M. Fedele, E. Franco, A. Paul, L. Silvestrini et al., *New Physics in $b \rightarrow s\ell^+\ell^-$ confronts new data on Lepton Universality*, [1903.09632](#).
 - [15] A. Datta, J. Kumar and D. London, *The B Anomalies and New Physics in $b \rightarrow se^+e^-$* , [1903.10086](#).
 - [16] J. Aebischer, W. Altmannshofer, D. Guadagnoli, M. Reboud, P. Stangl and D. M. Straub, *B -decay discrepancies after Moriond 2019*, [1903.10434](#).
 - [17] K. Kowalska, D. Kumar and E. M. Sessolo, *Implications for New Physics in $b \rightarrow s\mu\mu$ transitions after recent measurements by Belle and LHCb*, [1903.10932](#).

- [18] S. Descotes-Genon, J. Matias and J. Virto, *Understanding the $B \rightarrow K^* \mu^+ \mu^-$ Anomaly*, *Phys. Rev.* **D88** (2013) 074002 [[1307.5683](#)].
- [19] R. Gauld, F. Goertz and U. Haisch, *An explicit Z' -boson explanation of the $B \rightarrow K^* \mu^+ \mu^-$ anomaly*, *JHEP* **01** (2014) 069 [[1310.1082](#)].
- [20] A. J. Buras, F. De Fazio and J. Girrbach, *331 models facing new $b \rightarrow s \mu^+ \mu^-$ data*, *JHEP* **02** (2014) 112 [[1311.6729](#)].
- [21] W. Altmannshofer, S. Gori, M. Pospelov and I. Yavin, *Quark flavor transitions in $L_\mu - L_\tau$ models*, *Phys. Rev.* **D89** (2014) 095033 [[1403.1269](#)].
- [22] A. Crivellin, G. D'Ambrosio and J. Heeck, *Explaining $h \rightarrow \mu^\pm \tau^\mp$, $B \rightarrow K^* \mu^+ \mu^-$ and $B \rightarrow K \mu^+ \mu^- / B \rightarrow K e^+ e^-$ in a two-Higgs-doublet model with gauged $L_\mu - L_\tau$* , *Phys. Rev. Lett.* **114** (2015) 151801 [[1501.00993](#)].
- [23] A. Crivellin, G. D'Ambrosio and J. Heeck, *Addressing the LHC flavor anomalies with horizontal gauge symmetries*, *Phys. Rev.* **D91** (2015) 075006 [[1503.03477](#)].
- [24] C. Niehoff, P. Stangl and D. M. Straub, *Violation of lepton flavour universality in composite Higgs models*, *Phys. Lett.* **B747** (2015) 182 [[1503.03865](#)].
- [25] D. Aristizabal Sierra, F. Staub and A. Vicente, *Shedding light on the $b \rightarrow s$ anomalies with a dark sector*, *Phys. Rev.* **D92** (2015) 015001 [[1503.06077](#)].
- [26] A. Crivellin, L. Hofer, J. Matias, U. Nierste, S. Pokorski and J. Rosiek, *Lepton-flavour violating B decays in generic Z' models*, *Phys. Rev.* **D92** (2015) 054013 [[1504.07928](#)].
- [27] A. Celis, J. Fuentes-Martin, M. Jung and H. Serodio, *Family nonuniversal Z' models with protected flavor-changing interactions*, *Phys. Rev.* **D92** (2015) 015007 [[1505.03079](#)].
- [28] B. Allanach, F. S. Queiroz, A. Strumia and S. Sun, *Z' models for the LHCb and $g - 2$ muon anomalies*, *Phys. Rev.* **D93** (2016) 055045 [[1511.07447](#)].
- [29] D. Bećirević, O. Sumensari and R. Zukanovich Funchal, *Lepton flavor violation in exclusive $b \rightarrow s$ decays*, *Eur. Phys. J.* **C76** (2016) 134 [[1602.00881](#)].
- [30] A. Celis, W.-Z. Feng and M. Vollmann, *Dirac dark matter and $b \rightarrow s \ell^+ \ell^-$ with $U(1)$ gauge symmetry*, *Phys. Rev.* **D95** (2017) 035018 [[1608.03894](#)].
- [31] S. M. Boucenna, A. Celis, J. Fuentes-Martin, A. Vicente and J. Virto, *Non-abelian gauge extensions for B -decay anomalies*, *Phys. Lett.* **B760** (2016) 214 [[1604.03088](#)].
- [32] S. M. Boucenna, A. Celis, J. Fuentes-Martin, A. Vicente and J. Virto, *Phenomenology of an $SU(2) \times SU(2) \times U(1)$ model with lepton-flavour non-universality*, *JHEP* **12** (2016) 059 [[1608.01349](#)].
- [33] E. Megias, G. Panico, O. Pujolas and M. Quiros, *A Natural origin for the LHCb anomalies*, *JHEP* **09** (2016) 118 [[1608.02362](#)].
- [34] W. Altmannshofer, S. Gori, S. Profumo and F. S. Queiroz, *Explaining dark matter and B decay anomalies with an $L_\mu - L_\tau$ model*, *JHEP* **12** (2016) 106 [[1609.04026](#)].

- [35] A. Crivellin, J. Fuentes-Martin, A. Greljo and G. Isidori, *Lepton Flavor Non-Universality in B decays from Dynamical Yukawas*, *Phys. Lett. B* **766** (2017) 77 [[1611.02703](#)].
- [36] S. Di Chiara, A. Fowlie, S. Fraser, C. Marzo, L. Marzola, M. Raidal et al., *Minimal flavor-changing Z' models and muon $g - 2$ after the R_{K^*} measurement*, *Nucl. Phys. B* **923** (2017) 245 [[1704.06200](#)].
- [37] C.-W. Chiang, X.-G. He, J. Tandean and X.-B. Yuan, *$R_{K^{(*)}}$ and related $b \rightarrow s\ell\bar{\ell}$ anomalies in minimal flavor violation framework with Z' boson*, *Phys. Rev. D* **96** (2017) 115022 [[1706.02696](#)].
- [38] M. Crispim Romao, S. F. King and G. K. Leontaris, *Non-universal Z' from fluxed GUTs*, *Phys. Lett. B* **782** (2018) 353 [[1710.02349](#)].
- [39] L. Bian, H. M. Lee and C. B. Park, *B-meson anomalies and Higgs physics in flavored $U(1)'$ model*, *Eur. Phys. J. C* **78** (2018) 306 [[1711.08930](#)].
- [40] A. Falkowski, S. F. King, E. Perdomo and M. Pierre, *Flavourful Z' portal for vector-like neutrino Dark Matter and $R_{K^{(*)}}$* , *JHEP* **08** (2018) 061 [[1803.04430](#)].
- [41] D. Guadagnoli, M. Reboud and O. Sumensari, *A gauged horizontal $SU(2)$ symmetry and $R_{K^{(*)}}$* , *JHEP* **11** (2018) 163 [[1807.03285](#)].
- [42] B. Gripaios, M. Nardecchia and S. A. Renner, *Composite leptoquarks and anomalies in B-meson decays*, *JHEP* **05** (2015) 006 [[1412.1791](#)].
- [43] D. Bečirević, S. Fajfer and N. Košnik, *Lepton flavor nonuniversality in $b \rightarrow s\ell^+\ell^-$ processes*, *Phys. Rev. D* **92** (2015) 014016 [[1503.09024](#)].
- [44] I. de Medeiros Varzielas and G. Hiller, *Clues for flavor from rare lepton and quark decays*, *JHEP* **06** (2015) 072 [[1503.01084](#)].
- [45] R. Alonso, B. Grinstein and J. Martin Camalich, *Lepton universality violation and lepton flavor conservation in B-meson decays*, *JHEP* **10** (2015) 184 [[1505.05164](#)].
- [46] L. Calibbi, A. Crivellin and T. Ota, *Effective Field Theory Approach to $b \rightarrow s\ell\ell^{(\prime)}$, $B \rightarrow K^{(*)}\nu\bar{\nu}$ and $B \rightarrow D^{(*)}\tau\nu$ with Third Generation Couplings*, *Phys. Rev. Lett.* **115** (2015) 181801 [[1506.02661](#)].
- [47] G. Bélanger, C. Delaunay and S. Westhoff, *A Dark Matter Relic From Muon Anomalies*, *Phys. Rev. D* **92** (2015) 055021 [[1507.06660](#)].
- [48] R. Barbieri, G. Isidori, A. Pattori and F. Senia, *Anomalies in B-decays and $U(2)$ flavour symmetry*, *Eur. Phys. J. C* **76** (2016) 67 [[1512.01560](#)].
- [49] D. Bečirević, N. Košnik, O. Sumensari and R. Zukanovich Funchal, *Palatable Leptoquark Scenarios for Lepton Flavor Violation in Exclusive $b \rightarrow s\ell_1\ell_2$ modes*, *JHEP* **11** (2016) 035 [[1608.07583](#)].
- [50] D. Bečirević, S. Fajfer, N. Košnik and O. Sumensari, *Leptoquark model to explain the B-physics anomalies, R_K and R_D* , *Phys. Rev. D* **94** (2016) 115021 [[1608.08501](#)].

- [51] S. Sahoo, R. Mohanta and A. K. Giri, *Explaining the R_K and $R_{D^{(*)}}$ anomalies with vector leptoquarks*, *Phys. Rev.* **D95** (2017) 035027 [[1609.04367](#)].
- [52] G. Hiller, D. Loose and K. Schönwald, *Leptoquark Flavor Patterns & B Decay Anomalies*, *JHEP* **12** (2016) 027 [[1609.08895](#)].
- [53] P. Cox, A. Kusenko, O. Sumensari and T. T. Yanagida, *$SU(5)$ Unification with TeV-scale Leptoquarks*, *JHEP* **03** (2017) 035 [[1612.03923](#)].
- [54] A. Crivellin, D. Müller and T. Ota, *Simultaneous explanation of $R(D^{(*)})$ and $b \rightarrow s\mu^+\mu^-$: the last scalar leptoquarks standing*, *JHEP* **09** (2017) 040 [[1703.09226](#)].
- [55] Y. Cai, J. Gargalionis, M. A. Schmidt and R. R. Volkas, *Reconsidering the One Leptoquark solution: flavor anomalies and neutrino mass*, *JHEP* **10** (2017) 047 [[1704.05849](#)].
- [56] I. Doršner, S. Fajfer, D. A. Faroughy and N. Košnik, *The role of the S_3 GUT leptoquark in flavor universality and collider searches*, [1706.07779](#).
- [57] D. Buttazzo, A. Greljo, G. Isidori and D. Marzocca, *B-physics anomalies: a guide to combined explanations*, *JHEP* **11** (2017) 044 [[1706.07808](#)].
- [58] N. Assad, B. Fornal and B. Grinstein, *Baryon Number and Lepton Universality Violation in Leptoquark and Diquark Models*, *Phys. Lett.* **B777** (2018) 324 [[1708.06350](#)].
- [59] L. Di Luzio, A. Greljo and M. Nardecchia, *Gauge leptoquark as the origin of B-physics anomalies*, *Phys. Rev.* **D96** (2017) 115011 [[1708.08450](#)].
- [60] L. Calibbi, A. Crivellin and T. Li, *Model of vector leptoquarks in view of the B-physics anomalies*, *Phys. Rev.* **D98** (2018) 115002 [[1709.00692](#)].
- [61] M. Bordone, C. Cornella, J. Fuentes-Martin and G. Isidori, *A three-site gauge model for flavor hierarchies and flavor anomalies*, *Phys. Lett.* **B779** (2018) 317 [[1712.01368](#)].
- [62] M. Blanke and A. Crivellin, *B Meson Anomalies in a Pati-Salam Model within the Randall-Sundrum Background*, *Phys. Rev. Lett.* **121** (2018) 011801 [[1801.07256](#)].
- [63] D. Marzocca, *Addressing the B-physics anomalies in a fundamental Composite Higgs Model*, *JHEP* **07** (2018) 121 [[1803.10972](#)].
- [64] M. Bordone, C. Cornella, J. Fuentes-Martín and G. Isidori, *Low-energy signatures of the PS^3 model: from B-physics anomalies to LFV*, *JHEP* **10** (2018) 148 [[1805.09328](#)].
- [65] D. Bečirević, I. Doršner, S. Fajfer, N. Košnik, D. A. Faroughy and O. Sumensari, *Scalar leptoquarks from grand unified theories to accommodate the B-physics anomalies*, *Phys. Rev.* **D98** (2018) 055003 [[1806.05689](#)].
- [66] A. Crivellin, C. Greub, D. Müller and F. Saturnino, *Importance of Loop Effects in Explaining the Accumulated Evidence for New Physics in B Decays with a Vector Leptoquark*, *Phys. Rev. Lett.* **122** (2019) 011805 [[1807.02068](#)].
- [67] I. de Medeiros Varzielas and S. F. King, *$R_{K^{(*)}}$ with leptoquarks and the origin of Yukawa couplings*, *JHEP* **11** (2018) 100 [[1807.06023](#)].

- [68] L. Di Luzio, J. Fuentes-Martin, A. Greljo, M. Nardecchia and S. Renner, *Maximal Flavour Violation: a Cabibbo mechanism for leptoquarks*, *JHEP* **11** (2018) 081 [[1808.00942](#)].
- [69] T. Faber, M. Hudec, M. Malinský, P. Meinzinger, W. Porod and F. Staub, *A unified leptoquark model confronted with lepton non-universality in B-meson decays*, *Phys. Lett. B* **787** (2018) 159 [[1808.05511](#)].
- [70] J. Heeck and D. Teresi, *Pati-Salam explanations of the B-meson anomalies*, *JHEP* **12** (2018) 103 [[1808.07492](#)].
- [71] A. Angelescu, D. Bečirević, D. A. Faroughy and O. Sumensari, *Closing the window on single leptoquark solutions to the B-physics anomalies*, *JHEP* **10** (2018) 183 [[1808.08179](#)].
- [72] V. Gherardi, D. Marzocca, M. Nardecchia and A. Romanino, *Rank-One Flavor Violation and B-meson anomalies*, [1903.10954](#).
- [73] C. Cornella, J. Fuentes-Martin and G. Isidori, *Revisiting the vector leptoquark explanation of the B-physics anomalies*, [1903.11517](#).
- [74] C. Bobeth, A. J. Buras, A. Celis and M. Jung, *Patterns of Flavour Violation in Models with Vector-Like Quarks*, *JHEP* **04** (2017) 079 [[1609.04783](#)].
- [75] S.-P. Li, X.-Q. Li, Y.-D. Yang and X. Zhang, *$R_{D^{(*)}}, R_{K^{(*)}}$ and neutrino mass in the 2HDM-III with right-handed neutrinos*, *JHEP* **09** (2018) 149 [[1807.08530](#)].
- [76] C. Marzo, L. Marzola and M. Raidal, *Common explanation to the $R_{K^{(*)}}, R_{D^{(*)}}$ and ϵ'/ϵ anomalies in a 3HDM+ ν_R and connections to neutrino physics*, [1901.08290](#).
- [77] A. Crivellin, D. Müller and C. Wiegand, *$b \rightarrow s \ell^+ \ell^-$ Transitions in Two-Higgs-Doublet Models*, [1903.10440](#).
- [78] B. Gripaios, M. Nardecchia and S. A. Renner, *Linear flavour violation and anomalies in B physics*, *JHEP* **06** (2016) 083 [[1509.05020](#)].
- [79] P. Arnan, L. Hofer, F. Mescia and A. Crivellin, *Loop effects of heavy new scalars and fermions in $b \rightarrow s \mu^+ \mu^-$* , *JHEP* **04** (2017) 043 [[1608.07832](#)].
- [80] B. Barman, D. Borah, L. Mukherjee and S. Nandi, *Correlating the anomalous results in $b \rightarrow s$ decays with inert Higgs doublet dark matter and muon $(g-2)$* , [1808.06639](#).
- [81] B. Grinstein, S. Pokorski and G. G. Ross, *Lepton non-universality in B decays and fermion mass structure*, *JHEP* **12** (2018) 079 [[1809.01766](#)].
- [82] D. Bečirević and O. Sumensari, *A leptoquark model to accommodate $R_K^{\text{exp}} < R_K^{\text{SM}}$ and $R_{K^*}^{\text{exp}} < R_{K^*}^{\text{SM}}$* , *JHEP* **08** (2017) 104 [[1704.05835](#)].
- [83] J. F. Kamenik, Y. Soreq and J. Zupan, *Lepton flavor universality violation without new sources of quark flavor violation*, *Phys. Rev. D* **97** (2018) 035002 [[1704.06005](#)].
- [84] J. E. Camargo-Molina, A. Celis and D. A. Faroughy, *Anomalies in Bottom from new physics in Top*, *Phys. Lett. B* **784** (2018) 284 [[1805.04917](#)].
- [85] J. Aebischer, A. Crivellin, M. Fael and C. Greub, *Matching of gauge invariant dimension-six operators for $b \rightarrow s$ and $b \rightarrow c$ transitions*, *JHEP* **05** (2016) 037 [[1512.02830](#)].

- [86] S. Baek, *Dark matter contribution to $b \rightarrow s\mu^+\mu^-$ anomaly in local $U(1)_{L_\mu-L_\tau}$ model*, *Phys. Lett. B* **781** (2018) 376 [[1707.04573](#)].
- [87] J. Kawamura, S. Okawa and Y. Omura, *Interplay between the $b \rightarrow s\ell\ell$ anomalies and dark matter physics*, *Phys. Rev. D* **96** (2017) 075041 [[1706.04344](#)].
- [88] C.-W. Chiang and H. Okada, *A simple model for explaining muon-related anomalies and dark matter*, [1711.07365](#).
- [89] J. M. Cline and J. M. Cornell, *$R(K^{(*)})$ from dark matter exchange*, *Phys. Lett. B* **782** (2018) 232 [[1711.10770](#)].
- [90] S. Baek and C. Yu, *Dark matter for $b \rightarrow s\mu^+\mu^-$ anomaly in a gauged $U(1)_X$ model*, *JHEP* **11** (2018) 054 [[1806.05967](#)].
- [91] S. Baek, *Scalar dark matter behind $b \rightarrow s\mu\mu$ anomaly*, [1901.04761](#).
- [92] D. G. Cerdeño, A. Cheek, P. Martín-Ramiro and J. M. Moreno, *B anomalies and dark matter: a complex connection*, [1902.01789](#).
- [93] MUON G-2 collaboration, *Final Report of the Muon E821 Anomalous Magnetic Moment Measurement at BNL*, *Phys. Rev. D* **73** (2006) 072003 [[hep-ex/0602035](#)].
- [94] A. Crivellin, M. Hoferichter and P. Schmidt-Wellenburg, *Combined explanations of $(g-2)_{\mu,e}$ and implications for a large muon EDM*, *Phys. Rev. D* **98** (2018) 113002 [[1807.11484](#)].
- [95] F. del Aguila, J. de Blas and M. Perez-Victoria, *Effects of new leptons in Electroweak Precision Data*, *Phys. Rev. D* **78** (2008) 013010 [[0803.4008](#)].
- [96] K. Kannike, M. Raidal, D. M. Straub and A. Strumia, *Anthropic solution to the magnetic muon anomaly: the charged see-saw*, *JHEP* **02** (2012) 106 [[1111.2551](#)].
- [97] A. Joglekar, P. Schwaller and C. E. M. Wagner, *Dark Matter and Enhanced Higgs to Di-photon Rate from Vector-like Leptons*, *JHEP* **12** (2012) 064 [[1207.4235](#)].
- [98] J. Kearney, A. Pierce and N. Weiner, *Vectorlike Fermions and Higgs Couplings*, *Phys. Rev. D* **86** (2012) 113005 [[1207.7062](#)].
- [99] K. Ishiwata and M. B. Wise, *Phenomenology of heavy vectorlike leptons*, *Phys. Rev. D* **88** (2013) 055009 [[1307.1112](#)].
- [100] R. Dermisek and A. Raval, *Explanation of the Muon $g-2$ Anomaly with Vectorlike Leptons and its Implications for Higgs Decays*, *Phys. Rev. D* **88** (2013) 013017 [[1305.3522](#)].
- [101] K. Kowalska and E. M. Sessolo, *Expectations for the muon $g-2$ in simplified models with dark matter*, *JHEP* **09** (2017) 112 [[1707.00753](#)].
- [102] L. Calibbi, R. Ziegler and J. Zupan, *Minimal models for dark matter and the muon $g-2$ anomaly*, *JHEP* **07** (2018) 046 [[1804.00009](#)].
- [103] Z. Poh and S. Raby, *Vectorlike leptons: Muon $g-2$ anomaly, lepton flavor violation, Higgs boson decays, and lepton nonuniversality*, *Phys. Rev. D* **96** (2017) 015032 [[1705.07007](#)].
- [104] S. Raby and A. Trautner, *Vectorlike chiral fourth family to explain muon anomalies*, *Phys. Rev. D* **97** (2018) 095006 [[1712.09360](#)].

- [105] G. C. Branco and L. Lavoura, *On the Addition of Vector Like Quarks to the Standard Model*, *Nucl. Phys.* **B278** (1986) 738.
- [106] F. del Aguila, L. Ametller, G. L. Kane and J. Vidal, *Vector Like Fermion and Standard Higgs Production at Hadron Colliders*, *Nucl. Phys.* **B334** (1990) 1.
- [107] P. Langacker and D. London, *Mixing Between Ordinary and Exotic Fermions*, *Phys. Rev.* **D38** (1988) 886.
- [108] F. del Aguila, J. A. Aguilar-Saavedra and G. C. Branco, *CP violation from new quarks in the chiral limit*, *Nucl. Phys.* **B510** (1998) 39 [[hep-ph/9703410](#)].
- [109] MEG collaboration, *Search for the lepton flavour violating decay $\mu^+ \rightarrow e^+ \gamma$ with the full dataset of the MEG experiment*, *Eur. Phys. J.* **C76** (2016) 434 [[1605.05081](#)].
- [110] A. J. Buras, J. Girrbach-Noe, C. Niehoff and D. M. Straub, *$B \rightarrow K^{(*)} \nu \bar{\nu}$ decays in the Standard Model and beyond*, *JHEP* **02** (2015) 184 [[1409.4557](#)].
- [111] F. Gabbiani, E. Gabrielli, A. Masiero and L. Silvestrini, *A Complete analysis of FCNC and CP constraints in general SUSY extensions of the standard model*, *Nucl. Phys.* **B477** (1996) 321 [[hep-ph/9604387](#)].
- [112] J. A. Bagger, K. T. Matchev and R.-J. Zhang, *QCD corrections to flavor changing neutral currents in the supersymmetric standard model*, *Phys. Lett.* **B412** (1997) 77 [[hep-ph/9707225](#)].
- [113] J. Brod and M. Gorbahn, *The Z Penguin in Generic Extensions of the Standard Model*, [1903.05116](#).
- [114] A. Dedes, W. Materkowska, M. Paraskevas, J. Rosiek and K. Suxho, *Feynman rules for the Standard Model Effective Field Theory in R_ξ -gauges*, *JHEP* **06** (2017) 143 [[1704.03888](#)].
- [115] M. Algueró, B. Capdevila, S. Descotes-Genon, P. Masjuan and J. Matias, *Are we overlooking Lepton Flavour Universal New Physics in $b \rightarrow s \ell \ell$?*, [1809.08447](#).
- [116] LHCb collaboration, *Measurement of the ratio of branching fractions $BR(B_0 \rightarrow K^{*0} \gamma)/BR(B_{s0} \rightarrow \phi \gamma)$ and the direct CP asymmetry in $B_0 \rightarrow K^{*0} \gamma$* , *Nucl. Phys.* **B867** (2013) 1 [[1209.0313](#)].
- [117] LHCb collaboration, *Angular analysis of the $B^0 \rightarrow K^{*0} \mu^+ \mu^-$ decay using 3 fb^{-1} of integrated luminosity*, *JHEP* **02** (2016) 104 [[1512.04442](#)].
- [118] LHCb collaboration, *Angular analysis of the $B^0 \rightarrow K^{*0} e^+ e^-$ decay in the low- q^2 region*, *JHEP* **04** (2015) 064 [[1501.03038](#)].
- [119] LHCb collaboration, *Measurements of the S-wave fraction in $B^0 \rightarrow K^+ \pi^- \mu^+ \mu^-$ decays and the $B^0 \rightarrow K^*(892)^0 \mu^+ \mu^-$ differential branching fraction*, *JHEP* **11** (2016) 047 [[1606.04731](#)].
- [120] BELLE collaboration, *Lepton-Flavor-Dependent Angular Analysis of $B \rightarrow K^* \ell^+ \ell^-$* , *Phys. Rev. Lett.* **118** (2017) 111801 [[1612.05014](#)].
- [121] ATLAS collaboration, *Angular analysis of $B_d^0 \rightarrow K^* \mu^+ \mu^-$ decays in pp collisions at $\sqrt{s} = 8 \text{ TeV}$ with the ATLAS detector*, *JHEP* **10** (2018) 047 [[1805.04000](#)].

- [122] CMS collaboration, *Angular analysis of the decay $B^0 \rightarrow K^{*0} \mu^+ \mu^-$ from pp collisions at $\sqrt{s} = 8$ TeV*, *Phys. Lett. B* **753** (2016) 424 [[1507.08126](#)].
- [123] CMS collaboration, *Measurement of angular parameters from the decay $B^0 \rightarrow K^{*0} \mu^+ \mu^-$ in proton-proton collisions at $\sqrt{s} = 8$ TeV*, *Phys. Lett. B* **781** (2018) 517 [[1710.02846](#)].
- [124] W. Altmannshofer, P. Ball, A. Bharucha, A. J. Buras, D. M. Straub and M. Wick, *Symmetries and Asymmetries of $B \rightarrow K^* \mu^+ \mu^-$ Decays in the Standard Model and Beyond*, *JHEP* **01** (2009) 019 [[0811.1214](#)].
- [125] J. Matias, F. Mescia, M. Ramon and J. Virto, *Complete Anatomy of $\bar{B}_d^- \rightarrow \bar{K}^{*0} (- \rightarrow K \pi) l^+ l^-$ and its angular distribution*, *JHEP* **04** (2012) 104 [[1202.4266](#)].
- [126] S. Descotes-Genon, T. Hurth, J. Matias and J. Virto, *Optimizing the basis of $B \rightarrow K^* l l$ observables in the full kinematic range*, *JHEP* **05** (2013) 137 [[1303.5794](#)].
- [127] LHCb collaboration, *Angular analysis and differential branching fraction of the decay $B_s^0 \rightarrow \phi \mu^+ \mu^-$* , *JHEP* **09** (2015) 179 [[1506.08777](#)].
- [128] LHCb collaboration, *Test of lepton universality with $B^0 \rightarrow K^{*0} \ell^+ \ell^-$ decays*, *JHEP* **08** (2017) 055 [[1705.05802](#)].
- [129] M. Beneke, C. Bobeth and R. Szafron, *Enhanced electromagnetic correction to the rare B -meson decay $B_{s,d} \rightarrow \mu^+ \mu^-$* , *Phys. Rev. Lett.* **120** (2018) 011801 [[1708.09152](#)].
- [130] W. Altmannshofer, C. Niehoff and D. M. Straub, *$B_s \rightarrow \mu^+ \mu^-$ as current and future probe of new physics*, *JHEP* **05** (2017) 076 [[1702.05498](#)].
- [131] M. Misiak, A. Rehman and M. Steinhauser, *NNLO QCD counterterm contributions to $\bar{B} \rightarrow X_{s\gamma}$ for the physical value of m_c* , *Phys. Lett. B* **770** (2017) 431 [[1702.07674](#)].
- [132] M. Misiak et al., *Updated NNLO QCD predictions for the weak radiative B -meson decays*, *Phys. Rev. Lett.* **114** (2015) 221801 [[1503.01789](#)].
- [133] T. Hurth, E. Lunghi and W. Porod, *Untagged $\bar{B} \rightarrow X_{s+d} \gamma$ CP asymmetry as a probe for new physics*, *Nucl. Phys. B* **704** (2005) 56 [[hep-ph/0312260](#)].
- [134] BELLE collaboration, *Search for $B \rightarrow h \nu \bar{\nu}$ decays with semileptonic tagging at Belle*, *Phys. Rev. D* **96** (2017) 091101 [[1702.03224](#)].
- [135] D. Becirevic, M. Ciuchini, E. Franco, V. Gimenez, G. Martinelli, A. Masiero et al., *$B_d - \bar{B}_d$ mixing and the $B_d \rightarrow J/\psi K_s$ asymmetry in general SUSY models*, *Nucl. Phys. B* **634** (2002) 105 [[hep-ph/0112303](#)].
- [136] FERMILAB LATTICE, MILC collaboration, *$B_{(s)}^0$ -mixing matrix elements from lattice QCD for the Standard Model and beyond*, *Phys. Rev. D* **93** (2016) 113016 [[1602.03560](#)].
- [137] ETM collaboration, *B -physics from $N_f = 2$ tmQCD: the Standard Model and beyond*, *JHEP* **03** (2014) 016 [[1308.1851](#)].
- [138] D. King, A. Lenz and T. Rauh, *B_s mixing observables and $-V_{td}/V_{ts}$ from sum rules*, [1904.00940](#).
- [139] FLAVOUR LATTICE AVERAGING GROUP collaboration, *FLAG Review 2019*, [1902.08191](#).

- [140] PARTICLE DATA GROUP collaboration, *Review of Particle Physics*, *Phys. Rev.* **D98** (2018) 030001.
- [141] L. Di Luzio, M. Kirk and A. Lenz, B_s - \bar{B}_s mixing interplay with B anomalies, in *10th International Workshop on the CKM Unitarity Triangle (CKM 2018) Heidelberg, Germany, September 17-21, 2018*, 2018, [1811.12884](#).
- [142] L. Di Luzio, M. Kirk and A. Lenz, *Updated B_s -mixing constraints on new physics models for $b \rightarrow s\ell^+\ell^-$ anomalies*, *Phys. Rev.* **D97** (2018) 095035 [[1712.06572](#)].
- [143] MUON G-2 collaboration, *Muon ($g-2$) Technical Design Report*, [1501.06858](#).
- [144] J-PARC G-2/EDM collaboration, *A novel precision measurement of muon $g-2$ and EDM at J-PARC*, *AIP Conf. Proc.* **1467** (2012) 45.
- [145] T. P. Gorringe and D. W. Hertzog, *Precision Muon Physics*, *Prog. Part. Nucl. Phys.* **84** (2015) 73 [[1506.01465](#)].
- [146] A. Czarnecki, B. Krause and W. J. Marciano, *Electroweak Fermion loop contributions to the muon anomalous magnetic moment*, *Phys. Rev.* **D52** (1995) R2619 [[hep-ph/9506256](#)].
- [147] A. Czarnecki, B. Krause and W. J. Marciano, *Electroweak corrections to the muon anomalous magnetic moment*, *Phys. Rev. Lett.* **76** (1996) 3267 [[hep-ph/9512369](#)].
- [148] F. Jegerlehner and A. Nyffeler, *The Muon $g-2$* , *Phys. Rept.* **477** (2009) 1 [[0902.3360](#)].
- [149] K. Hagiwara, R. Liao, A. D. Martin, D. Nomura and T. Teubner, *$(g-2)_\mu$ and $\alpha(M_Z^2)$ re-evaluated using new precise data*, *J. Phys.* **G38** (2011) 085003 [[1105.3149](#)].
- [150] T. Aoyama, M. Hayakawa, T. Kinoshita and M. Nio, *Complete Tenth-Order QED Contribution to the Muon $g-2$* , *Phys. Rev. Lett.* **109** (2012) 111808 [[1205.5370](#)].
- [151] C. Gnendiger, D. Stöckinger and H. Stöckinger-Kim, *The electroweak contributions to $(g-2)_\mu$ after the Higgs boson mass measurement*, *Phys. Rev.* **D88** (2013) 053005 [[1306.5546](#)].
- [152] B. Chakraborty, C. T. H. Davies, P. G. de Oliveira, J. Koponen, G. P. Lepage and R. S. Van de Water, *The hadronic vacuum polarization contribution to a_μ from full lattice QCD*, *Phys. Rev.* **D96** (2017) 034516 [[1601.03071](#)].
- [153] F. Jegerlehner, *Muon $g-2$ theory: The hadronic part*, *EPJ Web Conf.* **166** (2018) 00022 [[1705.00263](#)].
- [154] M. Della Morte, A. Francis, V. Gülpers, G. Herdoíza, G. von Hippel, H. Horch et al., *The hadronic vacuum polarization contribution to the muon $g-2$ from lattice QCD*, *JHEP* **10** (2017) 020 [[1705.01775](#)].
- [155] M. Davier, A. Hoecker, B. Malaescu and Z. Zhang, *Reevaluation of the hadronic vacuum polarisation contributions to the Standard Model predictions of the muon $g-2$ and $\alpha(m_Z^2)$ using newest hadronic cross-section data*, *Eur. Phys. J.* **C77** (2017) 827 [[1706.09436](#)].
- [156] BUDAPEST-MARSEILLE-WUPPERTAL collaboration, *Hadronic vacuum polarization*

- contribution to the anomalous magnetic moments of leptons from first principles, *Phys. Rev. Lett.* **121** (2018) 022002 [[1711.04980](#)].
- [157] D. Giusti, F. Sanfilippo and S. Simula, *Light-quark contribution to the leading hadronic vacuum polarization term of the muon $g - 2$ from twisted-mass fermions*, *Phys. Rev.* **D98** (2018) 114504 [[1808.00887](#)].
- [158] D. Giusti, V. Lubicz, G. Martinelli, F. Sanfilippo and S. Simula, *Electromagnetic and strong isospin-breaking corrections to the muon $g - 2$ from Lattice QCD+QED*, [1901.10462](#).
- [159] RBC, UKQCD collaboration, *Calculation of the hadronic vacuum polarization contribution to the muon anomalous magnetic moment*, *Phys. Rev. Lett.* **121** (2018) 022003 [[1801.07224](#)].
- [160] A. Keshavarzi, D. Nomura and T. Teubner, *Muon $g - 2$ and $\alpha(M_Z^2)$: a new data-based analysis*, *Phys. Rev.* **D97** (2018) 114025 [[1802.02995](#)].
- [161] G. Colangelo, M. Hoferichter, M. Procura and P. Stoffer, *Dispersion relation for hadronic light-by-light scattering: theoretical foundations*, *JHEP* **09** (2015) 074 [[1506.01386](#)].
- [162] J. Green, O. Gryniuk, G. von Hippel, H. B. Meyer and V. Pascalutsa, *Lattice QCD calculation of hadronic light-by-light scattering*, *Phys. Rev. Lett.* **115** (2015) 222003 [[1507.01577](#)].
- [163] A. Gérardin, H. B. Meyer and A. Nyffeler, *Lattice calculation of the pion transition form factor $\pi^0 \rightarrow \gamma^* \gamma^*$* , *Phys. Rev.* **D94** (2016) 074507 [[1607.08174](#)].
- [164] T. Blum, N. Christ, M. Hayakawa, T. Izubuchi, L. Jin, C. Jung et al., *Connected and Leading Disconnected Hadronic Light-by-Light Contribution to the Muon Anomalous Magnetic Moment with a Physical Pion Mass*, *Phys. Rev. Lett.* **118** (2017) 022005 [[1610.04603](#)].
- [165] G. Colangelo, M. Hoferichter, M. Procura and P. Stoffer, *Rescattering effects in the hadronic-light-by-light contribution to the anomalous magnetic moment of the muon*, *Phys. Rev. Lett.* **118** (2017) 232001 [[1701.06554](#)].
- [166] T. Blum, N. Christ, M. Hayakawa, T. Izubuchi, L. Jin, C. Jung et al., *Using infinite volume, continuum QED and lattice QCD for the hadronic light-by-light contribution to the muon anomalous magnetic moment*, *Phys. Rev.* **D96** (2017) 034515 [[1705.01067](#)].
- [167] M. Hoferichter, B.-L. Hoid, B. Kubis, S. Leupold and S. P. Schneider, *Pion-pole contribution to hadronic light-by-light scattering in the anomalous magnetic moment of the muon*, *Phys. Rev. Lett.* **121** (2018) 112002 [[1805.01471](#)].
- [168] A. Kurz, T. Liu, P. Marquard and M. Steinhauser, *Hadronic contribution to the muon anomalous magnetic moment to next-to-next-to-leading order*, *Phys. Lett.* **B734** (2014) 144 [[1403.6400](#)].
- [169] G. Colangelo, M. Hoferichter, A. Nyffeler, M. Passera and P. Stoffer, *Remarks on higher-order hadronic corrections to the muon $g-2$* , *Phys. Lett.* **B735** (2014) 90 [[1403.7512](#)].
- [170] ALEPH, DELPHI, L3, OPAL, SLD, LEP ELECTROWEAK WORKING GROUP, SLD

- ELECTROWEAK GROUP, SLD HEAVY FLAVOUR GROUP collaboration, *Precision electroweak measurements on the Z resonance*, *Phys. Rept.* **427** (2006) 257 [[hep-ex/0509008](#)].
- [171] A. Efrati, A. Falkowski and Y. Soreq, *Electroweak constraints on flavorful effective theories*, *JHEP* **07** (2015) 018 [[1503.07872](#)].
- [172] J. De Blas et al., *HEPfit: a code for the combination of indirect and direct constraints on high energy physics models*, *Eur. Phys. J. C* **80** (2020) 456 [[1910.14012](#)].
- [173] A. Caldwell, D. Kollar and K. Kroninger, *BAT: The Bayesian Analysis Toolkit*, *Comput. Phys. Commun.* **180** (2009) 2197 [[0808.2552](#)].
- [174] ATLAS collaboration, *Search for supersymmetry in events with b -tagged jets and missing transverse momentum in pp collisions at $\sqrt{s} = 13$ TeV with the ATLAS detector*, *JHEP* **11** (2017) 195 [[1708.09266](#)].
- [175] ATLAS collaboration, *Search for squarks and gluinos in final states with jets and missing transverse momentum using 36 fb^{-1} of $\sqrt{s} = 13$ TeV pp collision data with the ATLAS detector*, *Phys. Rev.* **D97** (2018) 112001 [[1712.02332](#)].
- [176] ATLAS collaboration, *Search for electroweak production of supersymmetric particles in final states with two or three leptons at $\sqrt{s} = 13$ TeV with the ATLAS detector*, *Eur. Phys. J.* **C78** (2018) 995 [[1803.02762](#)].
- [177] CMS collaboration, *Search for new physics in events with two low momentum opposite-sign leptons and missing transverse energy at $\sqrt{s} = 13$ TeV*, .
- [178] A. Crivellin, G. D’Ambrosio, M. Hoferichter and L. C. Tunstall, *Violation of lepton flavor and lepton flavor universality in rare kaon decays*, *Phys. Rev.* **D93** (2016) 074038 [[1601.00970](#)].
- [179] C. Hambrock, A. Khodjamirian and A. Rusov, *Hadronic effects and observables in $B \rightarrow \pi \ell^+ \ell^-$ decay at large recoil*, *Phys. Rev.* **D92** (2015) 074020 [[1506.07760](#)].
- [180] A. J. Buras, M. Gorbahn, S. Jäger and M. Jamin, *Improved anatomy of ϵ'/ϵ in the Standard Model*, *JHEP* **11** (2015) 202 [[1507.06345](#)].
- [181] A. J. Buras, *ϵ'/ϵ -2018: A Christmas Story*, [1812.06102](#).
- [182] E. Pallante and A. Pich, *Strong enhancement of epsilon-prime / epsilon through final state interactions*, *Phys. Rev. Lett.* **84** (2000) 2568 [[hep-ph/9911233](#)].
- [183] V. Cirigliano, G. Ecker, H. Neufeld, A. Pich and J. Portoles, *Kaon Decays in the Standard Model*, *Rev. Mod. Phys.* **84** (2012) 399 [[1107.6001](#)].
- [184] T. Kitahara, U. Nierste and P. Tremper, *Supersymmetric Explanation of CP Violation in $K \rightarrow \pi\pi$ Decays*, *Phys. Rev. Lett.* **117** (2016) 091802 [[1604.07400](#)].
- [185] M. Endo, S. Mishima, D. Ueda and K. Yamamoto, *Chargino contributions in light of recent ϵ'/ϵ* , *Phys. Lett.* **B762** (2016) 493 [[1608.01444](#)].
- [186] A. Crivellin, G. D’Ambrosio, T. Kitahara and U. Nierste, *$K \rightarrow \pi\nu\bar{\nu}$ in the MSSM in light of the ϵ'_K/ϵ_K anomaly*, *Phys. Rev.* **D96** (2017) 015023 [[1703.05786](#)].

- [187] MUON G-2 collaboration, *Measurement of the Positive Muon Anomalous Magnetic Moment to 0.46 ppm*, *Phys. Rev. Lett.* **126** (2021) 141801 [[2104.03281](#)].
- [188] T. Aoyama et al., *The anomalous magnetic moment of the muon in the Standard Model*, *Phys. Rept.* **887** (2020) 1 [[2006.04822](#)].
- [189] LHCb collaboration, *Test of lepton universality in beauty-quark decays*, [2103.11769](#).
- [190] LHCb collaboration, *Angular analysis of the $B^+ \rightarrow K^{*+} \mu^+ \mu^-$ decay*, [2012.13241](#).